3-5-2008

Increasing Combat Aircraft Survivability Through Coherent Self-Protection Jammers

Soner Ozer

INCREASING COMBAT AIRCRAFT SURVIVABILITY THROUGH COHERENT SELF-PROTECTION JAMMERS

THESIS

Soner Özer, 1st Lt, TuAF

AFIT/GE/ENG/08-20

DEPARTMENT OF THE AIR FORCE
AIR UNIVERSITY

AIR FORCE INSTITUTE OF TECHNOLOGY

Wright-Patterson Air Force Base, Ohio

The views expressed in this thesis are those of the author and do not reflect the official policy or position of the Turkish Air Force, Department of Defense of the Republic of Turkey, the Republic of Turkey, United States Air Force, Department of Defense, or the United States Government.

AFIT/GE/ENG/08-20

INCREASING COMBAT AIRCRAFT SURVIVABILITY THROUGH COHERENT SELF-PROTECTION JAMMERS

THESIS

Presented to the Faculty

Department of Electrical and Computer Engineering

Graduate School of Engineering and Management

Air Force Institute of Technology

Air University

Air Education and Training Command

In Partial Fulfillment of the Requirements for the

Degree of Master of Science in Electrical Engineering

Soner Özer, BS

1st Lt, TuAF

March 2008

AFIT/GE/ENG/08-20

INCREASING COMBAT AIRCRFT SURVIVABILITY THROUGH COHERENT SELF-PROTECTION JAMMERS

Soner Özer, BS

1st Lt, TuAF

Approved:

_____/signed/_____	___5 March 2008_____
Michael A. Saville, Maj, USAF (Chairman)	Date
_____/signed/_____	___5 March 2008_____
Peter J. Collins, Civ, USAF (Member)	Date
_____/signed/_____	__5 March 2008_____
Andrew J. Terzouli, Civ, USAF (Member)	Date

Acknowledgments

I would like to express my cordial thanks to my thesis advisor and instructor, Michael A. Saville, for his excellent guidance throughout this research. The great motivation he inspired not only helped me to complete this scientific work on time but also provided me with the incentive to do more in the future. My special thanks go to my committee members, Andrew J. Terzuoli and Peter J. Collins, for their timely contributions to my research and for their generosity in sharing their superior experience in conducting scientific research. I should also express my gratitude for their friendship and hospitability which helped me and my family feel comfortable in a foreign country and increased my motivation further. I would also like to thank my instructor, Michael J. Havrilla, for everything I have learnt from his classes but especially for the general attitude to look for "the physical meaning" of everything I study. I should also acknowledge the crucial help I got from Paul A. Blue and Mathew W. Coldsnow for acquiring the flight path data I used in my thesis. Without their help this work would be incomplete. I also owe special thanks to Selami YILDIZ and Mehmet ULUBAY for their great help in doing the administrative work required for my papers and especially for their outstanding support throughout my education at AFIT.

Finally, I just would like to say a heartfelt "thank you" to my wife if nothing else just for her patience and love. This thesis is dedicated to her.

Table of Contents

Page

List of Figures

Page

List of Tables

Page

Abstract

When the battlefields were within the visual range, the objective of deception tactics in warfare was to deceive the human senses. In the battlefield of electromagnetic spectrum, the objective of deception is to deceive the sensors of the enemy weapon systems.

The survivability of the aircraft operating in hostile environment is of prime importance to the mission planner. If the aircraft can deny its location information to the tracking radar of the radar guided threat missile system, this, in return, may increase its survivability. The deception, a tactic which stems from the wisdom of ancient battles, incarnated in the form of Electronic Attack (EA) can give this capability to the aircraft operating in a hostile environment. Self-Protection Jammers (SPJs) mounted on aircraft that employ deception-repeater jamming techniques and the resulting effect of the deception jamming on the enemy sensor systems will be examined in this study.

The impact of the specific flight path and formation geometry should be considered both from the perspective of coherent SPJs effectiveness and the survivability. The individual effectiveness of the EA by SPJs is usually limited by the available Effective Radiated Power (ERP). Due to limitations on the size of the aircraft, one can not afford to build powerful SPJs. The jamming technique and the effect of multiple jammers with respect to jamming effectiveness need to be examined for mission planning

analysis. The specific jamming technique evaluated is the combined Range Gate Pull-Off (RGPO) and Velocity Gate Pull-Off (VGPO) against pulse Doppler radar.

The challenge is to decide the least vulnerable flight path and the formation geometry for a strike formation in an air-to-ground engagement scenario. The degree of survivability provided by the combination of the formation geometry, flight path and the EA (multiple spatially dispersed coherent jammers) is the focus of this research. The modeling and simulation of the interactions between the self-protection jammer and the pulse Doppler tracking radar with respect to formation geometry and flight path is the initial objective.

INCREASING COMBAT AIRCRAFT SURVIVABILITY THROUGH COHERENT SELF-PROTECTION JAMMERS

I. Introduction

"All warfare is based on deception. When near, make it appear you are far away, when far away, that you are near."

Sun-Tzu

In 2,500 years, nothing has changed with respect to warfare. In the battlefield of electromagnetic spectrum, the art of deception still holds a significant place. When the battlefields were within the visual range, the objective of deception tactics in warfare was to deceive the human senses. In the battlefield of electromagnetic spectrum, the objective of deception is to deceive the sensors of the enemy weapon systems.

In modern conventional warfare, tracking of targets in Beyond Visual Range (BVR) engagements is usually accomplished with tracking radars. The specifications of these tracking radars vary because they are designed to perform the tasks under various circumstances.

The surface-to-air radar guided missile systems are among the most formidable threats to the aircraft operating in hostile environment. These weapon systems rely on the target location information, which is provided by tracking radar, for the guidance of

its missiles [1]. Therefore, the deception of tracking radar paves the way for the success of avoiding the threat weapon system.

For range tracking, the time delay between the transmission of a radar pulse and the returned echo signal from the target is measured continuously. In addition to this time delay, the returned echo signal needs to be identified as a target as well [2]. The identification process for the returned echo signal is prone to deception by Electronic Attack (EA).

The range tracking errors which influence range measurements arise from thermal noise, range glint, radial acceleration, and calibration. A detailed discussion can be found in [1].

Self-protection EA systems tend to use deceptive EA techniques to break the lock of a tracking radar. The preference for deceptive EA technique over noise jamming technique stems from the fact that there is always a potential of tracking the noise jammer in angle or computing the range by using triangulation techniques. And this deficiency of noise jamming increases the vulnerability of the aircraft. The high efficiency of average transmitted power usage also favors the choice of deceptive EA techniques to be employed by the self-protection EA systems [3].

“Deception must never seem incongruous or illogical and should, where possible, accord with a pattern of events that the enemy has reason to expect” [4]. In this sense, the expectations of the sensor-to-be-deceived depend on its design characteristics. For instance, if the sensor is a pulse Doppler radar, then the deception attack should be planned with respect to the specific design parameters of pulse Doppler radars. In this

study the threat tracking radar is assumed to have typical design characteristics of a pulse Doppler radar.

Pulse Doppler radars generally utilize coherent transmission and reception. This means each transmitted pulse and the receiver local oscillator are synchronized to a highly stable oscillator. They employ coherent processing and this in return helps reject main-beam clutter [2].

The survivability of an aircraft operating in hostile environment is of prime importance to the mission planner. Survivability is defined as the "capability of a system, including its crew, to avoid or withstand a hostile environment without suffering an abortive impairment of its ability to accomplish its designated mission" [5]. If the aircraft can deny its location information to the tracking radar, this, in return, may increase its survivability. The deception, which stems from the wisdom of ancient battles, incarnated in the form of EA, can give this capability to the aircraft operating in a hostile environment. Self-Protection Jammers (SPJs) mounted on aircraft that employ deception-repeater jamming techniques will be examined in this study.

In the process of mission planning for an air-to-ground strike mission, one should decide the least vulnerable flight path and formation geometry of the aircraft to help increase the survivability of aircraft. The impact of the specific flight path and formation geometry should be considered both from the perspective of SPJ effectiveness and the survivability.

The effectiveness of the EA by SPJs is usually limited by the available Effective Radiated Power (ERP). Due to limitations on the size of the aircraft, one can not afford

to build powerful SPJs. The jamming technique and the effect of multiple jammers with respect to jamming effectiveness need to be examined for mission planning analysis.

Problem Statement

The challenge is to decide the least vulnerable flight path and the formation geometry for a strike formation in an air-to-ground engagement scenario. The degree of survivability provided by the combination of the formation geometry (multiple spatially dispersed jammers), flight path and the EA is the focus of this thesis. The modeling and simulation of the interactions between the self-protection jammer and the pulse Doppler tracking radar with respect to formation geometry and flight path is the initial objective.

Incentive for the Study

The emphasis on the survivability of the tactical aircraft increases for a set of reasons. These reasons include the fact that the average cost of a tactical aircraft increases due to the implementation of new and expensive technologies as a result of the requirements imposed by the advanced air defense threat systems. This need for an increased survivability for the tactical aircraft constitutes the basis on which this study is built. Also the fact that "operational requirements and budget constrains should require more cost-effectiveness out of modern EW suits and systems" [6] can be viewed as a supplementary incentive for this research since the research offers a solution to increase the EW effectiveness without increasing the overall cost.

Chapter II presents a literature review based on open literature. Most related and crucial information with regard to research is provided while a general level knowledge

of radar is assumed to be possessed by the reader. Chapter III describes the methodology used for the research. Chapter IV develops detailed mathematical model for the coherence of jamming signals and also includes an example of a jamming simulation. Chapter V focuses on the simulation of the tactical formation geometry and its respective EA effectiveness. Results, applications of the results and the recommendation on follow on work are discussed in Chapter VI.

II. Literature Review

Overview

Tactical mission planning for a strike mission is one of the most challenging tasks to which military pilots are exposed. Any useful guidelines or information related to mission planning may be vital in decreasing the cost of the strike for the friendly forces. The purpose of this literature review is to explore the available information that can be utilized in the process of building a mathematical model which can produce data useful for tactical strike mission planning.

The main conventional weapon systems that can be encountered as an air defense threat has a wide spectrum of variety. Although some general descriptions of these weapon systems can be found in open literature such as [7], [8], [9], and [1], the operational specifications of these systems and the tactics employed against such threats are typically classified. Therefore, the scope of the literature review is based on fundamental research methods without regard to specific radar systems or threats.

The background information provided in this chapter starts with a discussion on the sensors of weapon systems and gives an overview of pulse Doppler radar. The jamming technique examined in the tactical engagement modeling and the concept of combat survivability is also discussed.

Sensors of the Weapon Systems

Early applications of electronic systems in warfare starts from the applications of radio direction finder to give platform position and the application of radar to detect

hostile platform to increase the accuracy of artillery. The latest and the most lethal application is to use tracking radars in missile precision guidance and this application leaves any undefended platform with a small probability of survival in most cases [1].

The weapon employment process of any modern conflict usually starts with a detection phase and followed by the response phase. Detection phase for a missile system is conducted by a medium-range search radar (acquisition radar) and the response phase is conducted by the tracking radars and missile launchers. Therefore the victim sensors, the radar systems which are used in these phases, include search radar, tracking radar, missile seeker (radio-frequency seeker, infrared seeker), and electro-optic search systems [1]. In this study the victim sensor of interest is the tracking radar.

Tracking Radar

Tracking radars are assumed to be the primary threats, since they are considered to be associated with the terminal phases of the air defense missile systems. The primary mission of a tracking radar is to provide accurate information for missile guidance about the intended target's range, azimuth and elevation [1]. Tracking of an airborne target is usually accomplished by angle trackers and range trackers that are incorporated in tracking radars [3].

After the designation of target, tracking radar attempts to find and pursue the target in acquisition phase. In this acquisition phase, the range gate implemented by the radar is wider than the range gate in tracking phase [1].

The classic tracking radar follows the path of a single target and provides the measurement of its position in spherical coordinates. The position is tracked in angle and

range. The range tracking is accomplished by a servo controlled early-gate/late-gate range tracker in the radar receiver processor [3]. This closed loop automatic tracking is usually called split-gate tracking. The signal in each gate is integrated, and the difference between the amplitudes of the signals in each gate determines the way that the pair of the gates should move. When the difference of the signals is zero, the pair of the gates are considered to be centered and this position of the pair of the gates gives the range to the target [10]. The discrimination between targets in the same angle resolution cell can be accomplished with narrow range gates [3].

The time period for the analysis of the tactical engagement in this study is the tracking phase after the acquisition phase.

Radar Resolution

Radar observations are typically defined in four coordinates: azimuth angle, elevation angle, time delay (range), and frequency (Doppler shift, radial velocity). A target is considered to be resolved by the radar if the target signal can be separated from other target signals at least one of these coordinates [11]. Therefore if the target signal can not be separated from the other signals at any of these coordinates then it will be processed as a single target.

If the radar is employing an unmodulated pulse then the range resolution is simply limited with the pulse length. While the shorter unmodulated pulse will give better resolution, it will also decrease the energy conveyed by the pulse. One of the ways to overcome this limitation is pulse compression which is utilized in many modern radars. With pulse compression techniques, the required range resolution can be achieved

without sacrificing the pulse energy. In this study the assumption is made that the threat tracking radar is employing an unmodulated pulse and therefore the range resolution is given by,

$$\Delta R = \frac{c\tau}{2}. \quad (1)$$

Bandwidth of the receiving antenna Doppler filter and the antenna beam widths (azimuth and elevation) are the remaining factors that bound the radar resolution cell [11]. Therefore, with typical numbers the threat radar resolution cell boundaries can be defined for the modeling purposes.

Automatic Gain Control (AGC)

AGC is implemented in linear type receivers of tracking radars. AGC is needed for keeping the receiver always within its dynamic range and this is accomplished by compensating for the variations of target skin return power as a function of range, fluctuations due to target RCS and clutter [1]. Dynamic range is “the ratio, usually expressed in decibels, of the maximum to the minimum signal power over which a device can operate within some specified level of performance” [10].

Pulse Doppler (PD) Radar

In PD radar, the target velocity information is utilized in various processes including clutter rejection and solution of weapon-guidance equations.

> In pulsed Doppler radars, velocity discrimination provides a means of selecting the target while rejecting clutter within an angle-range resolution cell and also

> aids in the range tracking function by allowing the accurate prediction of future positions of the range gates. Generally, target velocity information is required in fire-control systems to solve the weapon-guidance equations. [3]

The design characteristics incorporated into tracking radars may include Electronic Protection (EP) capabilities. These capabilities may include low antenna sidelobes to reduce noise jamming power and pulse compression techniques to provide the corresponding processing gain to the radar signal while denying the processing gain to any mismatched jamming waveform. Detailed information on the EP capabilities of a typical tracking radar such as fast time constant, sensitivity time control, random PRF, frequency agility, moving target indicator, CFAR receiver, back-bias receiver, dicke-fix receiver, automatic frequency selection, sidelobe blanking, pulse compression and jammer strobe can be found in [1].

The EP protection capability of interest to this study is the coherent process employed by PD which makes it matched to the target Doppler and mismatched to the noncoherent jamming. This EP, which may be viewed as strength, has a disadvantage that can be exploited by deception jammer. The coherent process requires that the radar radiates for a relatively long time at a constant Radio Frequency (RF) and Pulse Repetition Frequency (PRF). This coherent dwell at a fixed RF and PRF can be exploited by a SPJ that employs deception EA tactics. These deception EA tactics are usually supported by digital RF memory (DRFM) that is used to emulate the coherent waveform [12], [1].

On the other hand in pulse Doppler processing, as a protection from deception jammers, the range data are differentiated (which gives range rate data) and compared

with the Doppler generated range rate data. This comparison allows discrimination against the deception jamming signals. Also, the acceleration data extracted from differentiation of the Doppler derived velocity data allows the discrimination of deception jamming signals with unrealistic accelerations [3], and [13].

The DRFM technology, as a replacement to the earlier application of recalculating memory loop which is not a coherent method of producing memory, provides the capability to employ EA tactics such as Range Gate Pull-Off against coherent radars more effectively [12].

Denial of the actual range rate information to the tracking radar of the threat system may cause an incoming radar guided missile to miss the target with a large miss distance where the miss distance is defined as the distance the missile detonates away from the SPJ.

In PD radar, the range gate's time position is varied by the expected Time of Arrival (TOA) of the pulse and the gate variation is conducted at a frequency less than the Doppler filter bandwidth (<1 kHz). Even though tracking of a pulse is not done in the conventional radar range tracking sense, the RGPO technique is equally applicable to the PD radar as well as conventional tracking radars [14].

Range-Gate Pull-Off (RGPO) and Velocity-Gate Pull-Off (VGPO)

RGPO is a deception EA technique described as below:

> The classic procedure initially employed by a deceptive SPJ against tracking radar is to transmit back an amplified replica of the radar waveform which captures the radar tracking loops. The signal then delayed in range at a rate which continuously increases, thus simulating a high-velocity accelerating target. At an appropriate time, the deceptive SPJ signal is removed, causing the tracking radar

> to lose range track with the last measured target position and velocity grossly in error. [15]

RGPO will not be effective in breaking the lock of PD tracking radar by itself [43], because, as stated earlier, the PD tracking radar will be checking the consistency of the two target range rate data sets obtained by the application of two different processes. The Doppler shift should also be incorporated in the repeated target signal to ensure the consistency between the Doppler derived range rate data and the range rate data derived from the differentiation of the target range data [3].

Leading edge range tracking combined with PRF jitter can also effectively deny any jammer attempting to employ RGPO as a deception jamming technique. But for PD tracking radar, implementation of PRF jitter in a pulse-to-pulse basis is not possible due to requirements of the Coherent Processing Interval (CPI). It is also possible for a jammer to implement very short delays (50 ns to 100ns) to minimize the capabilities of leading edge range trackers in rejecting the deceptive jamming signal pulses [3].

The jamming power requirement for effective RGPO can be expressed with regard to signal power from the actual target. Even though a Jamming-to-Signal (J/S) ratio of 40 dB is required for jamming the angle tracker of typical radar, a J/S ratio of 3 dB can be adequate to employ RGPO in many cases [14].

The total time for one pull-off cycle is typically 6 seconds and the pull-off program is generally parabolic in form. The rate of pull-off should also stay within the tracking capabilities of the victim radar. “Typical pull-off rates are on the order of three times the acceleration due to gravity (3 g), which is within the capability of most radar

tracking loops designed to operate against military targets" [14]. Therefore with typical parameters the total deception range can be found by using the formulation $r = \frac{1}{2}at^2$ which gives 529.2 m ($1.762\mu\text{sec}$).

If the effort by the jammer is identified as an attempt at deception by the victim radar, then the situation for the airborne platform carrying the jammer can be worse than no jamming [16].

The technique which includes the pseudo-Doppler shift in the repeated target signal to capture the tracking radar's velocity loop is called velocity gate pull-off (VGPO) [1]. Combination of the VGPO and RGPO can be viewed as the half of the total jamming effort necessary to break lock. This combination should be supported by another jamming effort aimed at breaking the angular track capability of hostile radar.

The effect of RGPO and VGPO can be analyzed based on the ambiguity function. For instance, "if the target return wave and RGPO jamming are within the ambiguity degree plot, then the radar cannot resolve the two signals. At this instant, RGPO is effective, for the radar range tracking wave gate locks on the jamming instead of the target" [17].

Combat Survivability

Combat survivability of aircraft has always been of interest to mission planners throughout the history of air warfare. The earlier belief that high performance military aircraft with transonic or supersonic speed were invulnerable to enemy air defenses has changed since the Vietnam War and the 1973 Arab-Israel War. The Egyptian and Syrian

air defense systems along with the synergy of missiles and guns (missile evasion maneuvers put the Israel aircraft in the effective range of MANPADS and light antiaircraft fire) caused Israel to lose 109 aircraft (%35 of its prewar inventory) in 9 days of war. In response to this new form of war, technological options adapted for military need and standoff precision attack, standoff jamming and finally low observables introduced into the theater. In 1991, during the opening night of Operation Desert Storm, 478 Suppression of Enemy Air Defense (SEAD), sweep and escort aircraft used techniques such as jamming, drones decoys and direct anti-radar missile attack and struck 144 targets at the cost of only one SEAD aircraft [18]. These facts confirm the impact of EW on the survivability.

One method to conceal the the approach of penetrating aircraft is to fly at very low altitudes to take advantage of the radar's inability to detect targets over the horizon. This method requires sophisticated navigation systems that are designed to enable the penetrating aircraft to maintain the desired route altitude until it reaches the designated target [14]. In Desert Storm, coalition forces lost thirty-eight aircraft and most of them were shot down because they persisted to fly low-level tactics for various reasons [19]. Therefore, it can be inferred that aircraft flying at medium or high altitude had a better survivability. But depending on the changing air defense environment, it is becoming less probable to increase the survivability of aircraft by just flying outside or above of the enemy airspace [20]. Therefore, it can be inferred that the exposure to threat weapon systems is inevitable and the need for increased survivability should be satisfied with

alternative approaches. The impact of the flight profile, specifically the altitude, is one of the considerations examined within the scope of this study.

Another method to conceal the approach of the penetrating aircraft can be discussed as

> Another method pursued that still receives much attention is the reduction of the echo power reflected from the protected vehicle, using special design techniques and absorptive coatings on the vehicle's reflecting surface; this approach is commonly known as the *stealth* technique. [14]

While this method is not within the scope of this study further discussions from the perspective of survivability can be found in [21].

Electronic Attack (EA) is the third method to conceal the penetrating aircraft [14] and this study is mainly concerned about the execution of this method and its impact on the survivability.

Survivability is defined as the capability of avoiding or withstanding threats in the tactical arena [22].

> The survival of a military aircraft operating in a hostile environment depends upon many diverse factors, such as the design of the aircraft, the skill and experience of the crew, the armament carried, the onboard countermeasures equipment, the off board supporting systems, and the tactics employed. [22]

The Self Protection Jammer (SPJ) falls in the category of onboard countermeasures that are designed to increase the survivability of the aircraft in a hostile environment.

Impact of EW and Flight Path on Survivability

Survivability can be further described by the terms *susceptibility* and *vulnerability*. Susceptibility is defined as "the degree to which a system is open to

effective attack due to one or more inherent weakness" [22]. It can also simply be defined as the inability of the aircraft to avoid a hit [23]. Vulnerability is defined as the inability of an aircraft to perform its assigned mission due to degradation caused by the exposure of the aircraft to man-made threat environment [3], [22]. In other words, vulnerability is the inability of the aircraft to withstand a hit [23]. Therefore, in order to increase survivability one should reduce the susceptibility and vulnerability of the aircraft. Reducing the ability of the enemy systems to see or hit the aircraft of friendly forces is the basic procedure for reducing susceptibility [24]. Reducing susceptibility can be achieved by passive signature reduction and active countermeasures. While signature reduction delays and degrades the acquisition process of threat system it also enhances jammer performance by increasing the ratio of jamming to signal (J/S) [25]. Nevertheless this study attempts to explore the active countermeasure procedures to increase the survivability by reducing susceptibility. One way to implement this procedure is to use onboard electronic attack equipment to degrade enemy tracking and missile guidance systems [22].

Recent studies argue that instead of improving one of the factors that affect survivability one should attempt to increase survivability through a "layered approach" [20] or an "onion skin approach" [26] and [6]. These approaches aim at improving a combination of factors on which the survivability depends as defined previously. A similar approach is attempted in this study as well.

In modern EW, the priorities of the self-protection systems can be discussed as:

> The first priority is to counter the approaching missile by increasing the missile's miss distance. The second priority is to deceive or to "break" the lock of threat's

> target acquisition sensor or fire control radar before launch, or even after launch, if the missile is semi active homing. The third priority is to counter the acquisition phase of the threat's fire-control radar trying to deny successful lock on. [6]

"Modern self protection concepts for mission survivability employ the outer protection layers of the onion" [6] where the outer layer can be described as flight route selection, mission planning, intelligence, signature reduction, terrain masking, countermeasures and Situational Awareness (SA) which is supported by self-protection systems. The common objective of these techniques is to avoid detection [26].

The second and the first priority concepts utilize SPJs as well as maneuvers and SA to avoid being hit [26] and [6].

The focus of the study is to explore the interaction between the effectiveness of electronic attack and various flight paths/geometries which can be visualized as a slice cut vertically from the "onion" discussed above. The ultimate outcome is expected to be an increase in survivability with the same equipment but different flight path and/or flight geometry. The effect of multiple jammers carried by the formation elements (multiple spatially dispersed jammers) is inspected from the perspective of coherency of the EA signals. Finally a survivability analysis is conducted.

Self-Protection Jammer (SPJ)

Self-protection jamming is an EA tactic in which the jammer is carried on the platform that is being tracked by the hostile radar. SPJs are usually the EA systems that repeat the received threat signal to deceive enemy electronic system. SPJs can also be in the form of noise jammers [15].

In modern applications, SPJs are usually integrated with Radar Warning Receivers (RWR) and provide automatic threat response. The threats identified by the RWR are also displayed to pilot throughout the process. Power management algorithms are used so as to match the countermeasures to the constantly changing threat picture. It is possible to use separate directional jammers on different parts of the aircraft to increase the spatial coverage of the jamming effort [9].

It is an important aspect of the SPJ that it must respond to the changes in the threat parameters as quickly as possible. In an optimum case, the SPJ should be able to reprogram itself during the engagement, even though the threat parameters are changing quickly. The tactical engagement scenarios examined in this study include aircraft with SPJ of deception-repeater type only.

In the modeling and simulation of this work, the type of jammer to be examined is chosen to be deception-repeater for the following reason:

> The deception jammer is most effective (as compared to the noise jammers) against modern radars which employ coherent integration techniques such as the pulsed Doppler and pulse-compression types. This occurs because radars employing coherent integration techniques have a large processing gain against noise (e.g. on the order of 20 to 60 dB), and hence attenuate the noise jammer signal by that amount, while necessarily accepting any target-like return unattenuated. [3]

In addition, deception jammers are more conservative in terms of power while "noise jammers tend to use a brute-blanket effect" [27] which usually require more power.

Every repeater jammer has an inherent time delay which can be described as the "time lapse between the reception of the radar signal by the receive antenna and the

radiation of transmission of the repeater output signal" [15]. This inherent time delay is typically 50ns to 100ns for repeater jammers [3]. This inherent delay is exploited by the radar designers in EP applications such as leading-edge tracking [14].

Tactical Formation

Basic two-ship formation, called an element, can be used as a building block for various optimization applications of tactics regarding tactical engagements because "most effective tactics build a division by combining two or more elements of two fighters" [28]. Building the campaign level engagement is usually achieved by the addition of formations in a hierarchical fashion based on the basic model of two-ship formation [29], and [30]. With a similar mindset basic two-ship formation is evaluated in the tactical scenarios explored in this study.

III. Methodology

Overview

Asking questions is the scientific way to start a research [31]. It helps define the research problem [32]. Defining the research problem can also be done by observation conducted in a questioning attitude [33]. With the utilization of these two approaches the question of "How can the survivability of a tactical aircraft formation be increased?" is asked to define the problem of this thesis.

Based on this question, the research hypothesis ("an imaginative preconception of a factual relationship" [33]) is postulated because without hypotheses, the scientific research becomes a mere collection of data [33].

Research Hypothesis

Survivability of a tactical aircraft formation can be increased by planning a proper formation geometry and flight path along with the employment of coherent self-protection jammers.

Analysis Method

The next scientific step is to test the hypothesis by experiment. In this case the experiment is the tactical engagement. Obviously setting up the actual tactical engagement for testing the hypothesis or observing an actual tactical engagement is not feasible within the scope of this research. Even though test flights can be designed for similar purposes it was not an option for this study. The available historical observation data about the actual tactical engagements in open literature are deemed inadequate in

technical detail. Therefore, the experiment to test the hypothesis is attempted to be conducted through mathematical modeling and computer simulation in a theoretical sense. The validation process of the models used in the experiment needs to be done as the follow on work to verify the results.

Using low cost simulations as an initial examination tool for tactical applications can be used effectively in many military applications [29], and [30]. This experiment through modeling and simulation should be viewed as a preliminary experiment which is designed to conserve resources. The positive results from a preliminary experiment can be viewed as a motivation to conduct more extensive experimentation [33].

The "method of difference" is utilized for developing the hypothesis. This method states "if an event is repeated with one factor but not another, the first factor is the causative agent" [33]. This method is implemented as a comparison and assessment of the resulting probabilities of survival of the two engagement scenarios. In the first scenario, SPJs are employed in a non-coherent fashion whereas in the second scenario they are employed in a coherent fashion. Quantitative models and simulations are used as part of this highly analytic research effort.

The outcome of the analytic research is expected to be the knowledge which is then processed by synthesis to generate understanding [26]. Synthesis is implemented as interpretation of the data arrived at the end of the experiment. The test of hypothesis is completed based on this understanding.

From the approach in [34] (shown in Fig. 1), the overall methodology of the analysis may be summarized as a study into the interaction (from the perspective of

survivability) between the factors of Electronic Warfare (EW) and flight path and geometry. Using modeling and simulation, two ship formations are studied to determine when and how self-protection jammers may be used coherently against tracking radar.

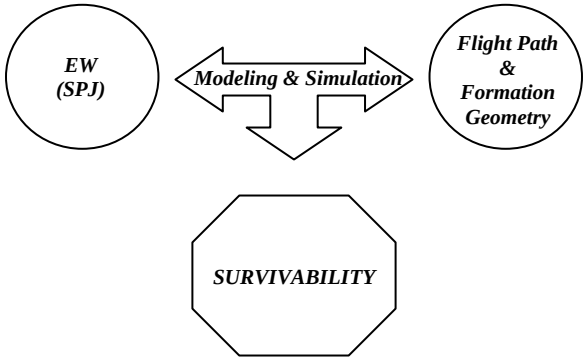

Figure 1: Overall analysis methodology [2].

Modeling and Simulation

In tactical engagement scenarios, the number of variables changing simultaneously usually presents a serious challenge for the modeling and simulation process. The designed model would possibly produce results only over a small part of the time period of interest [35]. The parameters of interest should therefore be chosen carefully. The modeling and simulation methodology is utilized from the perspective of EW. The resolution of the models is arranged with respect to their proposed impact on the EW concerns.

IV. Coherence of the Jamming Signals

Overview

Power and energy concepts are widely used as a measure of the signal size, and these concepts are discussed thoroughly in [36] and [37]. The coherence analysis is built upon the concepts of power and energy. The mathematical representation of the instantaneous and average power, and the energy of a signal are defined as [38]

$$\begin{aligned} &p_{inst}(t) = |s(t)|^2 \qquad (|s_1(t)+s_2(t)|^2 \neq s_1^2(t)+s_2^2(t),\ \textit{not additive}), \\ &p_{av}(t) = \frac{1}{T}\int_a^b p_{inst}(t)dt = \frac{1}{T}\int_a^b |s(t)|^2 dt \qquad T = b-a, \\ &E = \int_a^b p_{inst}(t)dt. \end{aligned} \tag{2}$$

As discussed in [39] and [40] “coherence” is described by how the signals constructively add in the receiver. When the pulse signal, which is radiated from a single jammer source, is observed at the output of the matched filter of the threat radar receiver, it is assumed to be at a constant energy level. When the second jammer signal is introduced, depending on the degree of constructive or destructive interference between the received jammer signals at the threat radar receiver, the energy level at the output of the matched filter may be higher or lower than the single jammer case. If the output energy level is higher than the single jammer case then the two spatially dispersed jammers are called “coherent”. If the output energy level is the same as or lower than the single jammer case, then the two jammers are called “incoherent” [39].

Further discussions on the characteristics of coherency can be found in [40]. For this study, the two jammer signals are considered to be of the same frequency, and the phase difference between the two jammer signals that arrive at the threat radar receiver is assumed to stem only from the Jamming Path Difference (JPD). JPD is evaluated as the primary cause for the Time Difference of Arrival (TDOA) between the two jamming pulse signals.

Deception Jamming J/S Equation Derivation

The size of the received jamming signal and the skin return signal can be represented as energy signals [41]. Time average of the received signal energy is referred to as the received power [36]. Therefore,

$$W = P_r \tau, \tag{3}$$

where τ is the pulse width and P_r is the peak power (watt) and W is energy. Peak power and the pulse width determine the energy of the pulse transmitted [42]. Setting $B_r = 1/\tau$ [43], Eq. 3 becomes,

$$W = \frac{P_r}{B_r}. \tag{4}$$

In an analogous manner jamming energy at the victim radar receiver will be given by

$$W_j = \frac{P_j}{B_j}. \tag{5}$$

The received power at the victim radar is given by [10]

$$P_r = \frac{P_t G_t}{4\pi R^2} \frac{\sigma}{4\pi R^2} A_e, \tag{6}$$

where the effective area of the victim radar receiving antenna A_e is defined as

$$A_e = \frac{G_t \lambda^2}{4\pi}, \tag{7}$$

assuming the radar is using the same antenna for transmit and receive. Then, for two way propagation Eq. (6) becomes

$$P_r = \frac{P_t G_t}{4\pi R^2} \frac{\sigma}{4\pi R^2} A_e (\Gamma^2 10^{-0.1\alpha L_j})(\Gamma^2 10^{-0.1\alpha L_j}), \tag{8}$$

where propagation loss factors are defined as follows [44]:

Γ : Propagation factor that takes into consideration the influence of the earth (underlying terrain) in the area between victim radar and the jammer.

(propagation factor that takes into consideration the influence of the earth (sea) beneath the path between the jammer and the radar.

α : Attenuation constant (dB/km)

L_j : attenuating portion of the path (km)

For the self-protection jamming case the jamming power at the victim radar is

$$P_j = \frac{P_j G_j}{4\pi R^2} A_e (\Gamma^2 10^{-0.1 L_j}). \tag{9}$$

Then, using Eq. (8) and Eq. (9), the J/S ratio (W_j / W_r) for self protection jammer case is

$$J/S = \frac{P_j G_j}{P_t G_t} \frac{4\pi R^2}{\sigma} \frac{1}{\Gamma^2} 10^{0.1L_j} \frac{B_r}{B_j} \gamma. \quad (10)$$

A polarization mismatch coefficient, γ, is also introduced to Eq. 10 since the application of random polarization in victim radars is a common practice [44]. Deception jamming waveforms mimic the skin return waveform therefore the bandwidth of the jamming signal is equal to the bandwidth of the skin return signal [43].

$$B_j = B_r. \quad (11)$$

Therefore, the final form of the J/S equation can be written as

$$J/S = \frac{P_j G_j}{P_t G_t} \frac{4\pi R^2}{\sigma} \frac{1}{\Gamma^2} 10^{0.1L_j} \gamma. \quad (12)$$

The J/S ratio is usually used for measuring the jammer effectiveness [45]. As the range, *R*, decreases the J/S decreases unless the ERP of the jammer is increased to compensate for the loss due to decreased range. The jamming power at the radar receiver can be increased by using multiple spatially dispersed coherent jammers. The mathematical development for jamming signals and the model for coherence are discussed next.

Pulse Signal Model

The pulse-Doppler (PD) radar is common, and has a simple mathematical model. Hence, the pulse-to-pulse analysis in this study is based on the PD radar. Various

mathematical models for various types of signals are discussed in the open literature [38], [45], [44], [46], [47], and the time-domain model of a deterministic signal is simply:

$$s(t) = a(t)\cos(\omega t + \theta)\,, \tag{13}$$

where $a(t)$, ω, θ represent the pulse envelope, angular frequency and initial phase of the signal. In a simple radar application, the signal represented by Eq. (13) is transmitted by the radar toward the target aircraft, reflects, and returns back to the radar receiver [45]. Notional transmitted and received pulses are shown in Fig. 2 where the transmitted pulse has peak amplitude A, initial phase of 0 degrees, and pulse duration, or width of τ - seconds. The received pulse is returned at time $2T_R$ where T_R is the one-way travel time to the target, and the amplitude is scaled according to the target's radar cross section and space loss.

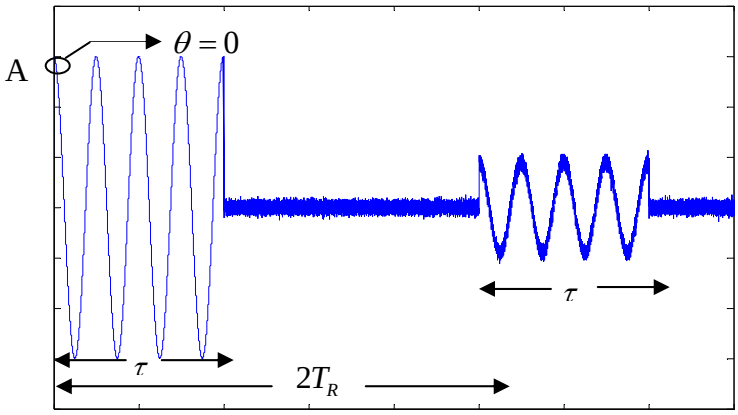

Figure 2: Simple voltage pulse representation.

Mathematical Models of the Jamming Signals

For detection of a signal whose parameters are known (with the exception of the delay), and the noise is Additive White Gaussian Noise (AWGN) the optimum detector

that can be used is a matched filter [48]. A matched filter is used in almost all radar receivers to maximize the output signal-to-noise ratio (SNR), and its derivation and implementation are discussed in detail in [10], [2], [11], and [48]. In the presence of white noise, the matched filter in the PD receiver produces maximum SNR, enabling target detection within each range bin, or cell. While Doppler processing is also used in the PD receiver, this study emphasizes EA against range tracking circuits. When multiple radar returns are received in the same range bin, their MF-output will either be enhanced or degraded. When false target signals appear in the range cell, range tracking is more complicated, but the effort here is to use multiple self-protection jammers in a quasi-coherent fashion to enhance detection of false targets from the jammers.

The matched filter output is the cross-correlation function of the transmitted and the received signal when no Doppler shift exists. When Doppler shift is present it is better to model the matched filter using Fourier Transform methods [10], but for convenience, the zero-Doppler signals are passed through the matched filter implemented as the correlation filter [10]:

$$y_{out}(t) = \int_{-\infty}^{+\infty} y_{in}(\lambda) h(t-\lambda) d\lambda, \tag{14}$$

where the matched filter input signal $y_{in}(t) = s(t) + n(t)$, $s(t)$ is the received signal, $n(t)$ is the receiver input noise, and assuming input SNR is large, $y_{in}(t) \approx s(t)$ [10]. Additionally, $h(t)$ is the matched filter's impulse response function and is designed such that $h(t) = s_{tx}(-t_k - t)$, where t_k corresponds to the kth range bin. Therefore, the matched

filter impulse response function of the radar receiver can be modeled with respect to Eq. (13) as

$$h(t) = A_0 \cos[\omega(-t_k - t) + \theta_0] = s_{tx}(-t_k - t). \tag{15}$$

In modern PD radar receivers, range tracking operates across all range bins making it convenient to define the phase term in Eq. (15) as

$$\theta_0 = \psi_0 - \omega t_k, \qquad k = 1, 2, ...K, \tag{16}$$

where $t_k = 2\tau k$ representing the starting time of the *k*th range bin, and ψ_0 is the initial phase.

The received skin-return and the false target signals from the target platforms are expressed similarly to Eqs. (13) and (16) as

$$s_s(t) = A_s \cos(\omega t + \theta_s), \tag{17}$$
$$s_1(t) = A_1 \cos(\omega t + \theta_1), \tag{18}$$
$$s_2(t) = A_2 \cos(\omega t + \theta_2), \tag{19}$$

where θ_s, θ_1 and θ_2 and are

$$\theta_s = \theta_0 + \delta_s, \tag{20}$$
$$\theta_1 = \theta_0 + \delta_1, \tag{21}$$
$$\theta_2 = \theta_0 + \delta_2, \tag{22}$$

and $\delta_1 = \omega(t_1 - t_k)$, $\delta_2 = \omega(t_2 - t_k)$ and $\delta_s = \omega(t_s - t_k)$. Time of Arrival (TOA) of the signal from the first jammer is t_1 and the TOA of the second jammer signal is t_2. A summary of the mathematical models for the signals defined so far is given in Table 1.

Table 1: Summary of the mathematical models of the signals.

SIGNAL	MODEL
Transmitted Signal	$s_{tx}(t) = A_0 \cos(\omega t + \psi_0)$
Matched Filter Impulse Response Function	$h(t) = A_0 \cos(-\omega t + \psi_0 - \omega t_k)$
Skin Return Signal (Unresolved Echo for kth range bin)	$s_s(t) = A_s \cos[\omega t + \psi_0 - \omega t_k + \omega(t_s - t_k)]$
Jamming Signal From Jammer #1	$s_1(t) = A_1 \cos[\omega t + \psi_0 - \omega t_k + \omega(t_1 - t_k)]$
Jamming Signal From Jammer #2	$s_2(t) = A_2 \cos[\omega t + \psi_0 - \omega t_k + \omega(t_2 - t_k)]$

Model for Coherence

The power of the matched filter output can be compared to a threshold to determine when the two jamming signals achieve success. It should be noted that this approach is also valid for velocity-gate jamming.

The graphical illustration of the radar range bin and the ideal received signal pulses are shown in Fig. 3. The convolution process is indicated by the sliding reference pulse. The TOAs for the skin return signal, signal from Jammer #1 and the signal from Jammer #2 are marked as t_s, t_1 and t_2 respectively. The *k*th range bin starting time is marked t_k. The range bin length equals pulse width τ and bandwidth β is

$$\beta = \frac{1}{\tau}. \tag{23}$$

In the tactical flight formation, the term “Jammer #1” refers to the self-protection jammer mounted on the leader aircraft and “Jammer #2” refers to the self-protection jammer mounted on the wingman. Each self-protection jammer emits the same waveform with the same initial phase. This may be accomplished by using a common reference clock. In addition, the jamming antennas are modeled as isotropic sources, so that only TDOA affects the signals upon arrival at the receiver. Finally, it is assumed that the lead aircraft is closest in range to the tracking radar in the engagement scenarios making the specific order of the arrival times of the three pulse signals:

$$\tau < (t_k = t_s) \leq t_1 \leq t_2 \leq PRI\,. \tag{24}$$

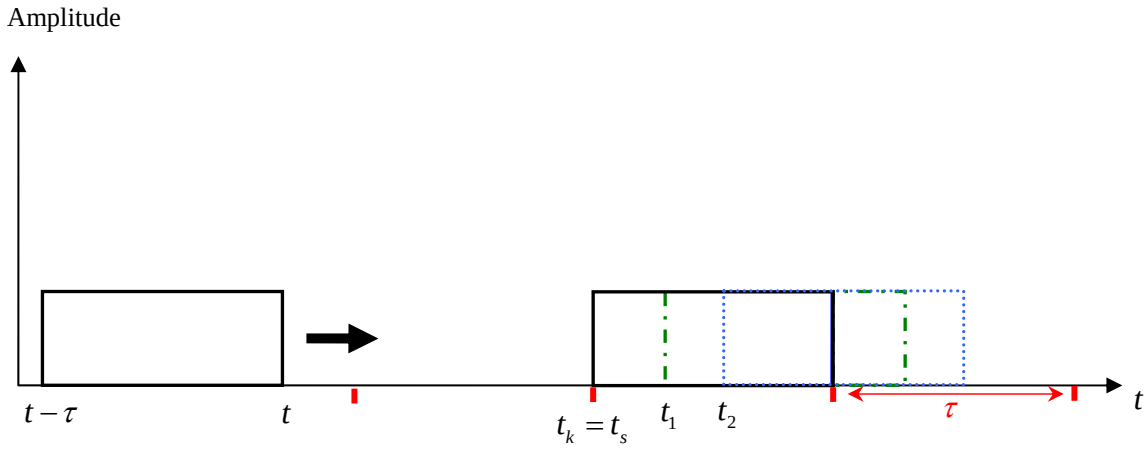

Figure 3: Analytic representation of the input pulses, the convolution process and the range bin representation.

Simulation of Coherence

Based on the mathematical derivation outlined previously, the matched filter output for the specific range bin is simulated. Pulse width τ is set to $1\,\mu\text{sec}$.

In Figure 4a, TDOA= τ so the jamming pulse signals from two jammers appear in separate, but adjacent range bins. The normalized instantaneous power and the energy levels [36] in each range bin are equal (ignoring a slight difference due to sampling) because the two jamming pulse signals are modeled as identical signals.

In Figure 4b, the two signals overlap in range bin #1 by 53% causing the increased MF-output in range bin #1 while the MF-output of range bin #2 decreases.

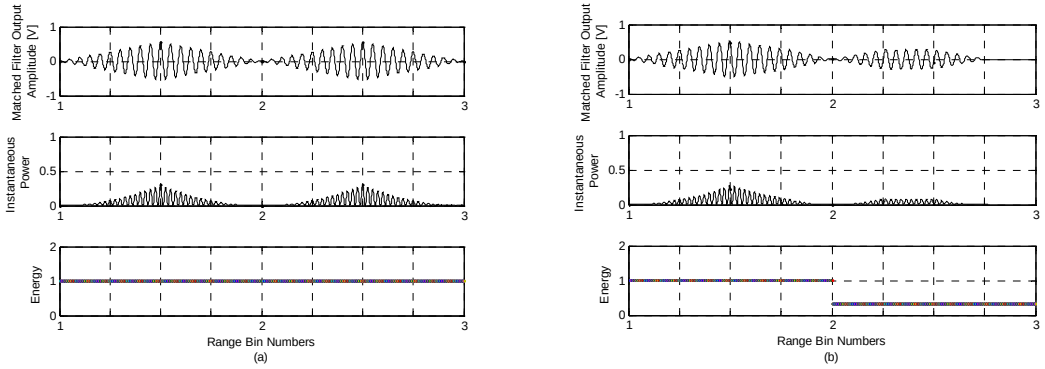

Figure 4: Power and the energy analysis of the matched filter output for the specific range bin.

As seen in Fig. 4, the MF-output oscillates, making the coherency oscillatory at best. In the general case, noise and aircraft flight dynamics make TDOA and coherency statistical in nature.

Figure 5 illustrates how the energy level in the first range bin (power integrated over τ) varies with respect to different TDOA values when the intermediate frequency is set to 10 MHz. For other frequencies, the energy level will still be bounded by the ideal matched filter envelope [10] making coherence probabilistic. When the two jamming pulse signals arrive at the exact same time, TDOA=0 and the maximum energy level is achieved in the range bin. Yet, as TDOA increases until TDOA $\geq \tau$, the MF-output is

equivalent to a single pulse return. In other words, the desired single false target appears as two distinct false targets depicted in Fig. 4a. While multiple false targets may be tactically useful, the EA goal is to induce a strong false target in a single range bin.

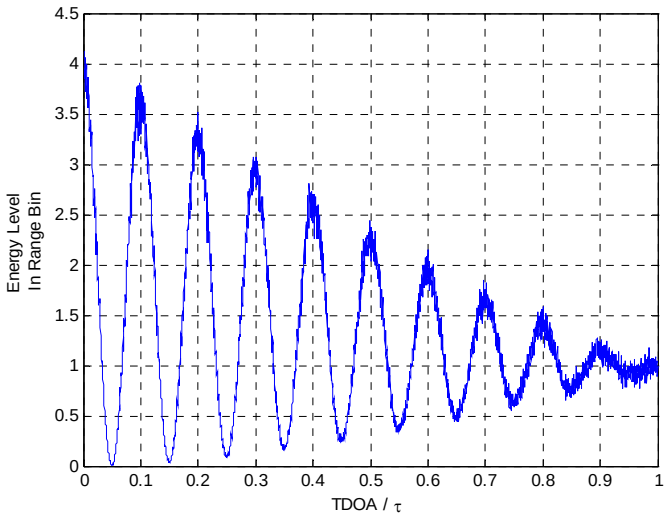

Figure 5: Total energy levels in the kth range bin with respect to different TDOAs.

RGPO Simulation

An analytical simulation is given below with the typical jamming parameters given in [15]. In Figure 6, an A-Scope representation of PD tracking radar is simulated. The echo (skin return) of the aircraft formation of two ships is shown in Fig. 6a. The formation aircraft are separated by 110 m, and a constant radial airspeed of 300 m/s is chosen for both aircraft throughout the simulation. Flight path starts 80 km away from the tracking radar site. The pulse width (τ) for the radar is, $\tau = 1\mu s$ (radar range resolution is 150 m). So the tracking radar is unable to resolve the two ship formation as seen in Fig. 6a.

With the onset of the coherent jamming signals from SPJs, the AGC circuitry of the tracking radar is captured and the AGC level is raised during the dwell time. This is shown in Fig. 6b.

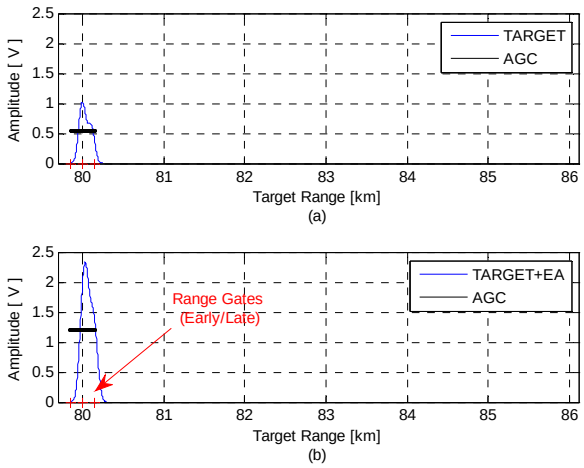

Figure 6: RGPO dwell time.

After the dwell time, the deception jamming signal is delayed gradually with a modified exponential walk function during the total walk time.

In Fig. 7b, the range gates are observed at the simulation time of $t = 0.8$ sec and they are tracking the deception signal instead of the target formation. AGC level is also observed as slightly higher than the skin return of the target formation. This is the desired result out of the total coherent EA signal power at the victim radar receiver. At this simulation the total coherent EA signal power is 1.7 times higher than the skin return signal power of the formation. The coherency of the jamming signals is assumed to be 100% so they perfectly add together.

The inevitable initial delay of the repeater delay is used as 150 nsec and total walk off time is 10 μsec with a total walk time of 5 sec [15]. Both targets assumed to have identical nonfluctuating RCS values of 2 m^2.

In Fig. 7a, the target formation echo is shown as it is being tracked by the range gates. The initial RGPO walk is also depicted in Fig. 7b where the range gates are observed as tracking the jamming signal.

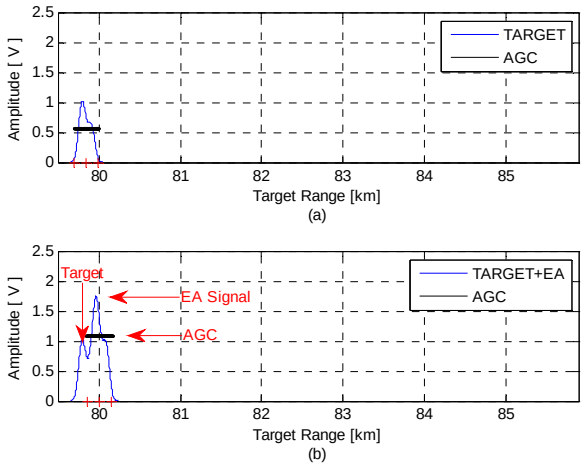

Figure 7: Initial RGPO walk.

In Fig. 8, the successful RGPO is observed with snapshots from the total walk time. At the end of the total walk time the EA signal is turned off and a new RGPO cycle is initiated after a short time interval.

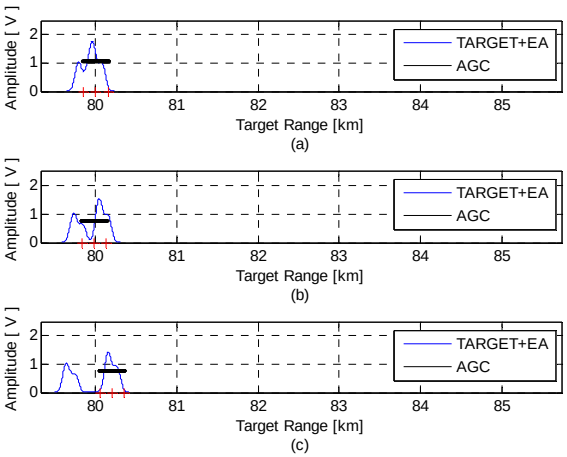

Figure 8: Snapshots from RGPO walk time.

If the effort by the SPJ is identified as an attempt to deceive by the victim radar, then the situation for the airborne platform carrying the SPJ can be worse than if it had used no jamming [12]. Therefore, the parameters of jamming such as the total walk time, walk rate and dwell time should be planned for each threat individually. The deception waveform parameters should also match the reflected waveform parameters in an optimum fashion.

Summary

The derivation of J/S equation for deception SPJ is given in the beginning of the chapter. Based on this equation, it is seen that the J/S ratio can be increased by increasing the jamming power at the victim radar. The analysis for coherence of jamming signals revealed that for certain intervals of TDOA, the resulting jamming power at the victim radar is higher than the single jammer case due to coherence. Therefore, the TDOA of the jamming signals need to be evaluated for different tactical formations and flight paths.

RGPO simulation is also illustrated as an example for the application of a typical jamming technique and the importance of the jamming signal power analysis. Evaluation of the TDOA for different tactical formations and flight profiles are discussed in the next chapter.

V. Tactical Scenario

Overview

Because every tactical engagement has its own characteristics, it is highly unlikely to find a general survivability solution that can be considered valid for every engagement scenario [27]. For example, single stand-off jamming intentionally removes the jamming platform from the threat engagement zone, whereas self-protection jamming is based on an immediate threat to survivability [22]. Therefore the mutual aspects of the factors affecting survivability, which are discussed in Chapter II, should be evaluated for the very specific engagement of interest. For the tactical scenario where two or more aircraft execute the strike mission, these factors should also be evaluated with respect to mutual support within aircraft formation.

The intention of this study is to explore the interactions between the tactical formation flight geometry and the theoretical effectiveness of coordinated on-board countermeasures. Subsequently this data may be useful for mission planning with the expectation of increased survivability of the tactical formation.

An overall discussion about the general tactical engagement scenario from a single aircraft point of view and the threat avoidance tactics such as flying low and fast can be found in [7] while a detailed discussion especially about an engagement in target area is provided in [8]. However, the tactical scenario chosen for this study is of a specific and decisive time period to investigate survivability. Tactical consideration is placed on the survivability of the formation instead of a single aircraft.

Tactical Scenario Considerations and Assumptions

A threat analysis process may be considered as an appropriate starting point for the description of a realistic tactical mission scenario. This analysis generally depends on intelligence data gathered by appropriate means. Open sources may also provide intelligence for theoretical analysis. For instance, an air defense threat capability map from a global perspective can be found in [20] where the different levels of expected air defense threat are marked with regard to different countries.

Even though the threat weapon system in the scenario is assumed to be a fixed Surface-to-Air Missile (SAM) system the overall model is designed so that it can also be converted to an air-to-air tactical engagement scenario. The missile guidance is assumed to be accomplished only by tracking radar of coherent pulsed Doppler type and the terrain of the engagement is considered to be plain and having no significant effect or limitation on the overall evaluation.

The deception tactic can be used to degrade the state of readiness of the enemy weapon system [20] which then may allow to apply the so-called principle of "the best defense is to avoid detection" [1]. But this perspective of deception is not evaluated and the weapon systems are considered to be alert and ready to fire.

Despite the fact that "intimate intelligence database for each threat and for each threat-mode is required in order to generate effective techniques" [6], the threat missile specifications and the missile performance are not modeled but the missile is assumed to be using command guidance. The distinction between the different guidance systems of missiles is usually related to their designed missions. Medium-to-long range missiles (50-

150 km) are designed for local area defense and tend to utilize semiactive homing or active homing guidance. On the other hand medium-to-long range missiles are designed for defending a target of great value and tend to utilize beam-riding or command guidance [1]. Further classifications of the missile guidance systems are discussed in [49] and [50] such as preset guidance and terrestrial guidance including beam rider, command guidance and seeker or homing guidance.

In command guidance, two separate tracking radars track the missile and the target simultaneously. The target and missile states are fed to a central computer for the calculation of the missile trajectory for successful interception. The calculated missile trajectory commands are then transmitted to the missile [2]. The victim radar for the EA in the engagement scenario is the coherent pulsed Doppler tracking radar that is assumed to be tracking the target for the missile guidance.

When no EA is present, the rms target-to-missile miss distance of a command guidance missile at range R is given by [1]

$$m_d = \sqrt{\varepsilon_{tgt}^2 + \varepsilon_{msl}^2}, \tag{25}$$

where ε_{tgt} is the precision of the radar that is tracking the target while ε_{msl} is the precision of the radar tracking the missile. The objective of range deception jamming may be viewed as an attempt to increase the ε_{tgt} value described above. Further discussion on the precision of target tracking can be found in [1].

Alternatively, it is also possible to use a single radar in command guidance systems. This type of guidance is called “command-to-line-of-sight” missile guidance

and the missile is commanded to stay within the radar beam throughout the engagement. More detailed information on command guidance and the calculation of miss distance in this type of guidance can be found in [1], [49], and [50].

Typical airborne active and passive countermeasure systems include chaff/flare/decoy dispenser systems, self-protection or escort radar jammers, Directional Infra-Red Counter Measures and stealth, and may be integrated with a RWR or similar equipment for the automatic response to a threat in tactical arena [9]. The specific employment procedures are not the focus of this research. Hence, this study focuses on SPJ systems that employ deception jamming techniques, the impact of the flight geometry on the mutual jamming effort of the tactical strike formation and the resulting degree of survivability.

While "it is not uncommon to find chaff and active EA used simultaneously in certain cases" [27], the study focuses on only active EA in this regard within the scope of the scenario described above. One disadvantage with the chaff employment is the fact that it may be impossible for the tactical aircraft to carry enough chaff for the complete duration of the mission. Therefore, if the operational information about the correct time to dispense chaff is not available, then the reliance on chaff may present a deficiency [27].

Aircraft Position Error

The deterministic positions of the aircraft for any time during the flight profile are represented as

$$\vec{r}_1 = \hat{x}x_1(t) + \hat{y}y_1(t) + \hat{z}z_1(t),$$
$$\vec{r}_2 = \hat{x}x_2(t) + \hat{y}y_2(t) + \hat{z}z_2(t), \qquad (26)$$

where the origin of the coordinate system is at the victim radar site, making $JPD_{\text{det}} = \left|\vec{r}_2\right| - \left|\vec{r}_1\right|$ deterministic. However, the actual position of the aircraft may be slightly different than the desired position because of calibration error of the navigation instruments, inaccuracy in available navigation data, pilot error, instabilities in the atmosphere and so on. Therefore, in a rigorous way, if we assume that the maximum probable position error is equal for all three axes and has a Gaussian distribution with zero mean and variance σ_p^2, then the actual position of the aircraft can be anywhere, but the highest probability is for position near the desired flight path. It is also reasonable to approximate the distribution as uniform making the position vary within a sphere and with equal probability. The sphere's center is the intended position of the aircraft and the radius of the sphere is the maximum probable position error. This position error should be accounted for all the aircraft in the formation.

This random position error is simulated as Δ_{JPD} and the actual jamming path difference is

$$JPD_{actual} = JPD_{\text{det}} + \Delta_{JPD} \qquad (27)$$

Note that this random position error Δ_{JPD} can be included in Eq. (26) for each axis, but is easily included as a one-dimensional variable because $\left|\vec{r}_1\right|$ and $\left|\vec{r}_2\right|$ will change

with the same distribution. This approach is also easily verifiable with telemetry or measured position data.

The sample space for Δ_{JPD} is limited to the interval $[a,b]$ with zero mean and $a=-b=$ maximum position error (as a vector magnitude). Therefore, the sample space for JPD_{actual} is simply shifted as $\Omega_{JPD}=[JPD_{\det}+a, JPD_{\det}+b]$. As stated previously, TDOA is assumed to result from JPD only. Therefore, it is possible to map from JPD_{actual} to $TDOA_{actual}$ by scaling Eq. (27) by the speed of light, c, as

$$\begin{aligned} TDOA_{rand} &= \frac{1}{c}(JPD_{\det}+\Delta_{JPD}), \\ &= TDOA_{\det}+\Delta_{TDOA}, \end{aligned} \tag{28}$$

Figure 9 illustrates the sample space for Ω_{TDOA} when uniformly distributed, but this approach is suitable for Gaussian or other distributions. This sample space is used in the following section to compute the probability of coherence.

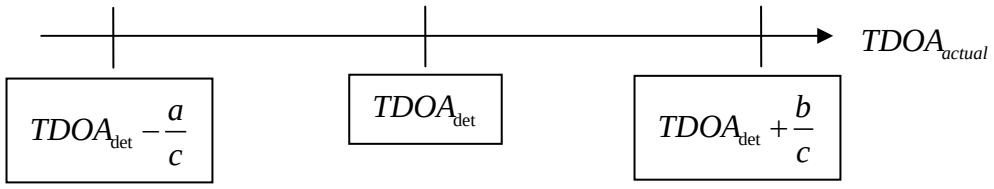

Figure 9: Sample space (continuous) for random variable $TDOA_{actual}$.

Probability of Coherence

Due to the assumption that aircraft position error has a uniform distribution, and receiver noise is a Gaussian random process [10], the resulting coherence of the jamming signals need to be defined as a random process. Keeping in mind the assumption that the

jamming signal from Jammer #1 arrives at the beginning of the range bin, we define the event $\mathbb{C}$ as

$\mathbb{C}$: Both jamming signals arrive in the same range bin of interest, i.e. $0 \le TDOA_{actual} \le \tau$, and they are coherent according to the definition in Section 2.0. In other words, the resulting range bin energy exceeds the threshold set for coherency.

From the previous discussion, TDOA is a random process that can be defined by a probability density function, and Fig. 5 displays the conditional probability density function for coherency given TDOA. Therefore, the probability of coherence is [51]

$$P[\mathbb{C}] = \int_{\Omega_{actual}} [\mathbb{C} \mid \lambda][\lambda] d\lambda, \tag{29}$$

where $[\mathbb{C} \mid \lambda]$ and $[\lambda]$ are the probability density functions and the integration interval is shown in Fig. 9.

Two-Ship Formations

Two-ship formation can be described as "a team of two fighters acting in concert against the adversary" [52]. In this formation, one of the aircraft is designated as leader and the second aircraft is designated as wingman. Depending on the tactics to be employed for the specific mission, geometry of the formation varies. In line abreast formation wingman flies directly abeam the leader while in trail formation wingman flies directly behind the leader. The basic principle of the formation is the mutual support of the aircraft within the formation. Further information on the formation types such as fighting wing, echelon, and fluid formation can be found in [52].

Trail Formation

The two-ship formation flying in trail and the jamming paths of the individual aircraft are depicted in Fig. 10. The formation is assumed to be perfectly aligned with the threat radar x-axis. The altitudes and radial velocities of the two aircraft are exactly the same. The distance marked as dx in Fig. 10 is the trail distance between the elements of the formation that is of importance for the mission planning process.

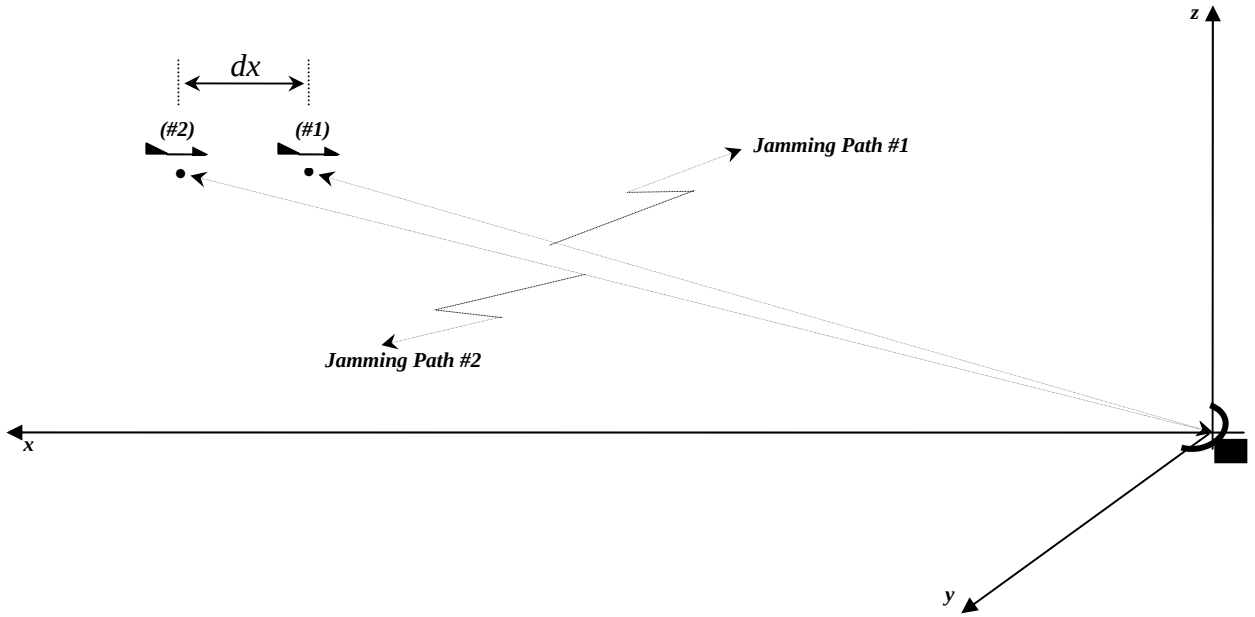

Figure 10: Tactical Scenario Case #1.

Finding the Probability of Coherence

The two-ship formation flying in trail and the jamming paths of the individual aircraft are depicted in Fig. 10. The $TDOA_{\text{det}}$ is given by the chart in Fig. 11 for various altitudes and trail distances, dx.

The chart shows results for the scenario where the lead aircraft is at 15 NM lateral distance from the threat radar. If the formation is flying at 10 000 feet with a trail distance of 300 feet then from Fig. 11, $TDOA_{\text{det}}$ equals $0.606\,\mu\text{sec}$. When the maximum probable position error is 100 feet then the sample space for $TDOA_{actual}$ is $\Omega_{TDOA} = [0.5044, 0.7076]$. With this flight path and formation geometry $P[\mathbb{C}] = 0.595$.

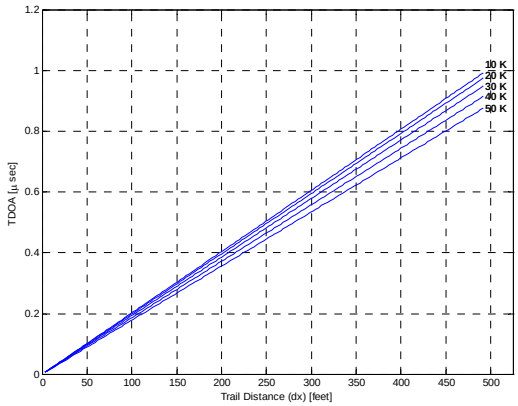

Figure 11: Charts for $TDOA_{\text{det}}$ interval analysis for case #1.

Line abreast Formation

In this case, lead aircraft is perfectly aligned with the threat radar x-axis while the wingman is flying at the parallel flight path at the same altitude with same radial velocity. This scenario is depicted in Fig. 13 where the individual jamming paths are also shown.

The distance marked as *dy* in Fig. 13 is the line abreast distance that is of importance for mission planning.

Finding the Probability of Coherence

The $TDOA_{\text{det}}$ for various altitudes and various *dy* values are given in Fig. 12. The chart is drawn for the scenario where the lead aircraft is at 15 NM lateral distance from the threat radar. If the formation is flying at 10 000 feet with a line abreast distance of 5000 feet, then from Fig. 12 $TDOA_{\text{det}}$ equals $0.2768\,\mu\text{sec}$. When the maximum probable position error is 100 feet, $\Omega_{TDOA} = [0.1752, 0.3784]$.

Similarly, this flight path and formation geometry results in $P[\mathbb{C}] = 0.635$.

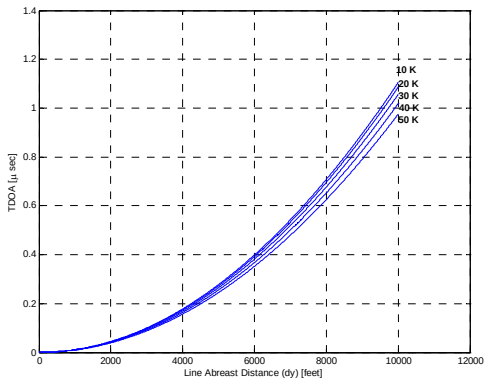

Figure 12: TDOA with respect to different line abreast distances.

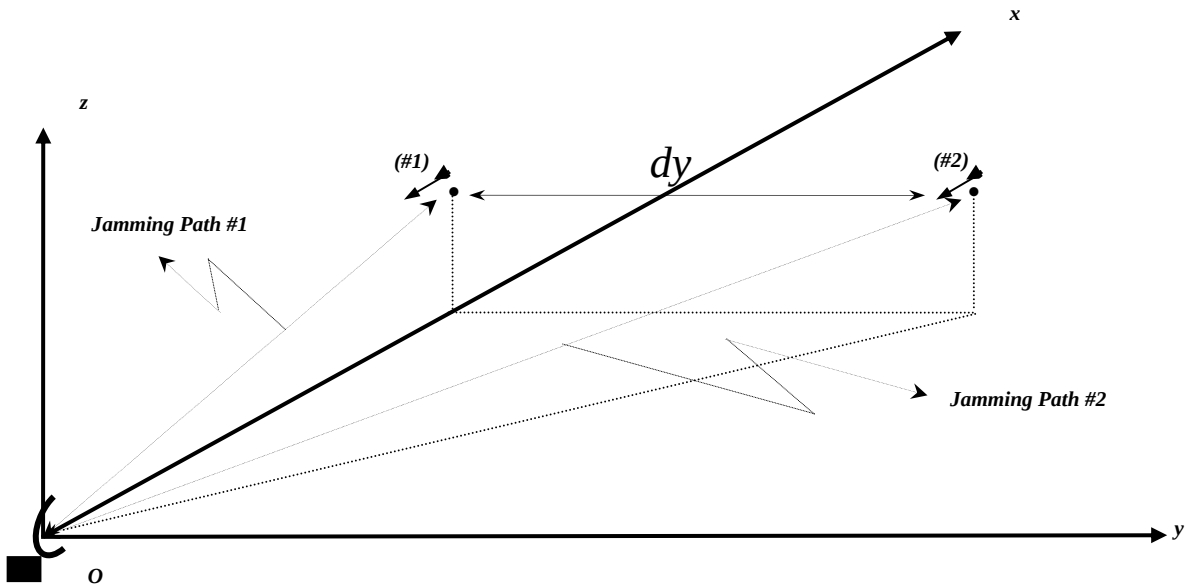

Figure 13: Tactical scenario case #2.

Flight Profile Simulation and Coherence

Based on the examples explained in previous sections, six flight profiles with different parameters are evaluated. The primary design objective of the flight profile simulations is to evaluate the impact of the trail and line-abreast distance on the probability of coherence of the jamming signals. Based on the analysis of coherence, results are evaluated from the perspective of survivability.

Flight Simulation

The flight simulation model, a six-degrees-of-freedom nonlinear aircraft model which is used for flight profile trials in this study, was developed by Maj. Paul A. Blue and Maj. Mathew W. Coldsnow at Air Force Institute of Technology (AFIT) [53]. The F-16 simulation model is based on the book "Aircraft Control and Simulation", 2nd Edition, by B. Stevens and F. Lewis. As mentioned in reference above, the F-16 model uses the data from NASA-Langley wind tunnel tests [54] on a subscale model of an F-16 airplane. Flight simulation is primarily designed for preliminary evaluation of flight tests.

In the first of three profiles, the initial formation type is set as trail formation while line-abreast formation is used for the remaining three flight profiles. A 20-degree check turn is initiated by the formation during the simulation and this turn is designed to allow the evaluation of a third formation geometry called fighting wing formation. This type of formation geometry is discussed in [52].

Aircraft position error is simulated in three axes by the addition of Gaussian position error with zero mean. Maximum position error (variation) is assumed to be 25

feet. Fluctuations in the flight paths of individual aircraft due to position error can be seen in Fig. 14.

For all six profiles evaluated below, victim radar is assumed to be operating at a PRF of 1000 Hz and the total simulation time is fixed at 154 seconds. These parameters yielded a total of 154 000 pair of pulses for the entire profile.

Profile #1

In this profile, two-ship trail flight formation is used. The trail distance, dx, is set as 250 feet. Flight parameters for Profile #1 are given in Table 2.

Table 2: Parameters for profile #1.

PROFILE #1 TRAIL	Airspeed First Leg (1.5 min)	Airspeed Second Leg (1 min)	Altitude (feet)	Turn Rate (for 20° check turn)	Trail Distance 'dx' (feet)
Leader	450 K	450 K	20 000	5 deg/min	
Wingman	450 K	450K	20 000	5 deg/min	250

Trail formation geometry used for the simulation is shown in Fig. 14 as a snapshot from the actual simulation. This visualization is taken from the beginning of the first leg.

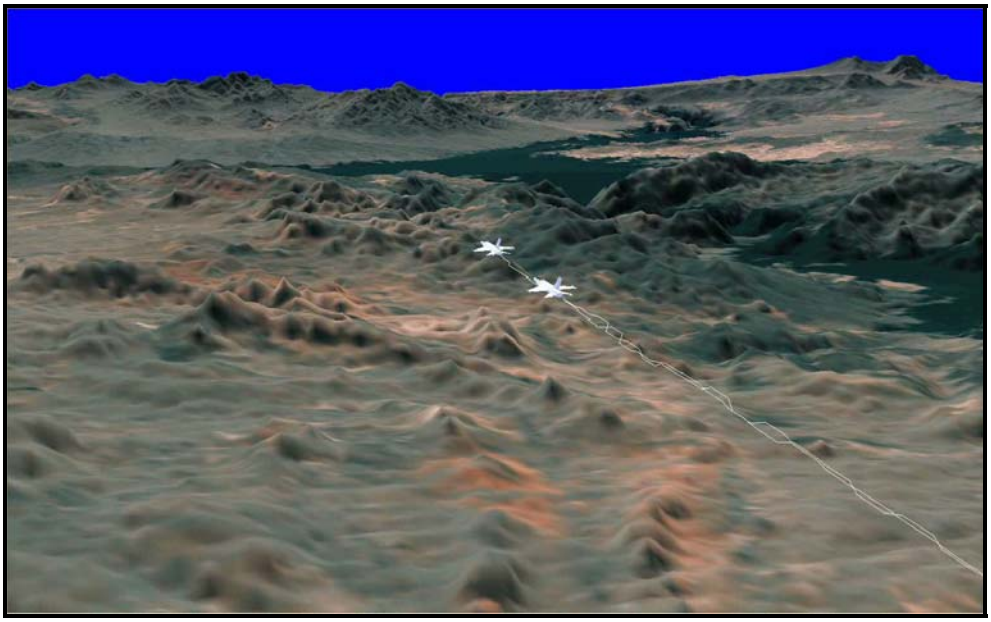

Figure 14: A snapshot from the beginning of the actual flight profile simulation for visualization of the trail formation geometry [53].

The top view of the flight profile flown is given in Fig. 15. Starting position is chosen 25 NM away from the victim radar. Victim radar location is defined as the origin for the simulation. Total flight profile lasted 154 seconds. The first leg is flown for 90 seconds followed by a 20-degree check turn which is completed in 4 seconds. The second leg is flown for 60 seconds.

Both aircraft initiated the check turn at time $t = 90\,\mathrm{s}$ and the top view of the flight profile containing the turn is enlarged in Fig. 16 for clarification of the fighting wing formation in the second leg.

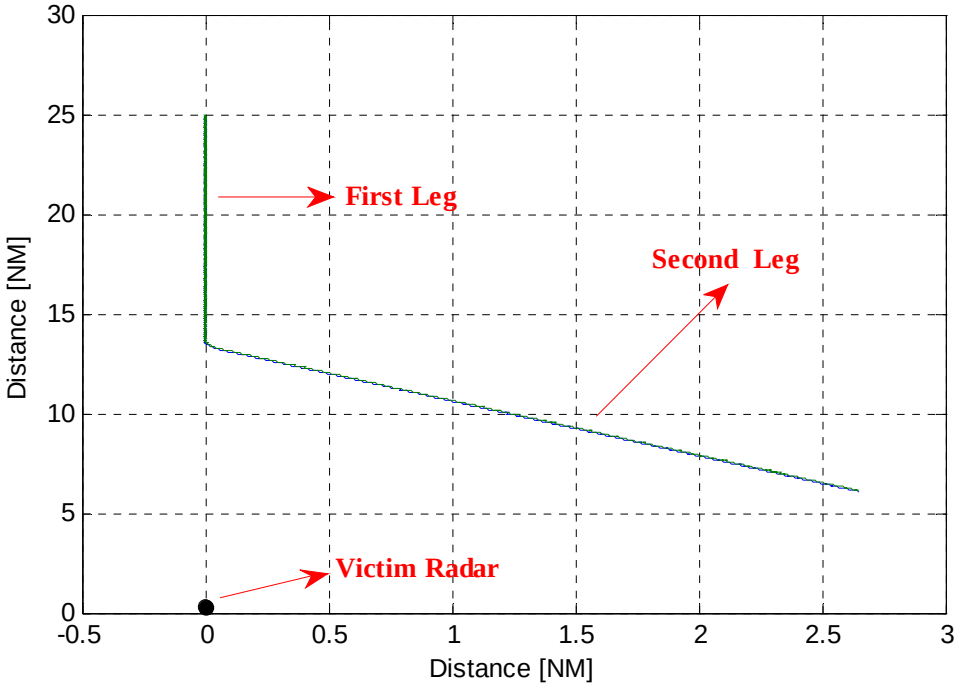

Figure 15: Top view for the complete profile #1.

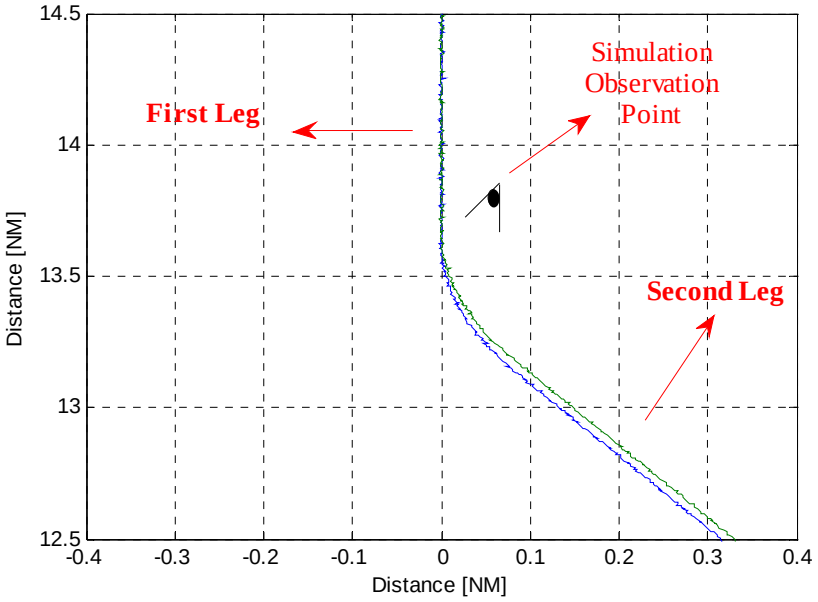

Figure 16: Check turn flight profile top view zoomed.

A simulation snapshot during the turn is given in Fig. 17a and the observation point for this snapshot is shown in Fig. 16. Note that both aircraft initiate the turn at the same time which results in the fighting wing formation as shown in Fig. 17b.

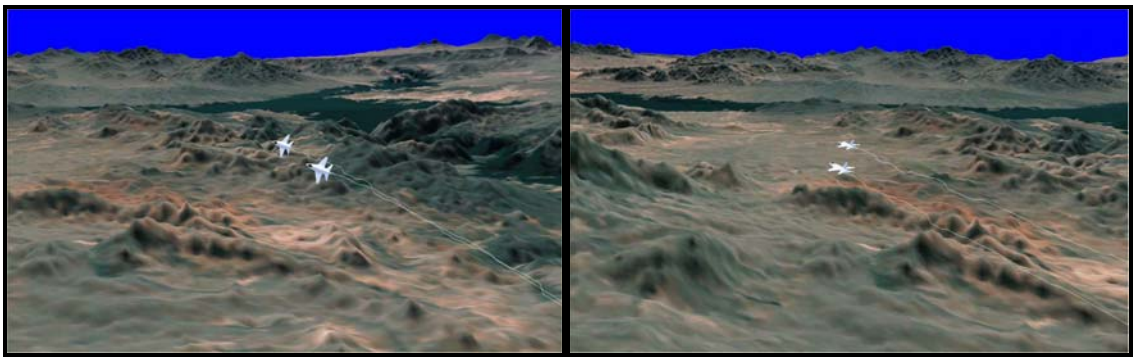

(a) (b)

***Figure 17: Check turn and the trail formation changes to fighting wing formation* [53].**

The coherence of jamming signals for the complete profile is evaluated. Using the coherence model that is developed in Chapter IV, the total energy levels for the 154 000 pair of pulses are found and shown in Fig. 18. A summary of the resulting coherence is given below Fig. 18. When the TDOA is greater than the range bin width, pulses arrive in different range bins. These pulses are referred to as “separate pulses”. In this flight geometry, all pair of pulses stayed within the range bin of interest; thus, the value for the number of separate pair of pulses is zero. Note that the total energy after the turn increased when the formation geometry is fighting wing. The probability of coherence is given by the ratio of the number of pulse pairs to the total number of pulse pairs. Therefore, $P[C] = 0.78$ is found with the results given below Fig. 18. A Probability Density Function (PDF) is also given in

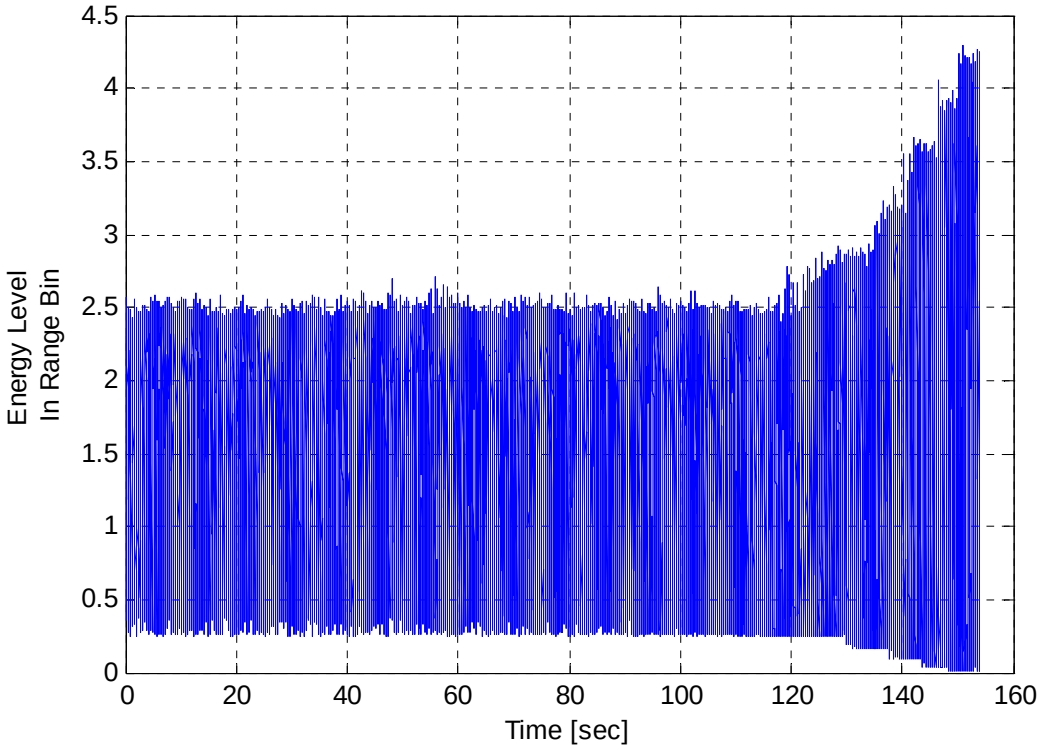

Figure 18-Energy levels in the range bin of interest for each pair of pulses during profile#1 (Number of coherent pair of pulses= 120091, Number of noncoherent pair of pulses= 33909, Number of separate pair of pulses= 0, Number of total pair of pulses=154000).

For the observation of the distribution of the total energy levels in the range bin of interest, probability density function for the 250 feet trail formation is given in Fig. 19. Note that $P[C]$ can be calculated for different threshold values. Energy levels in the x-axis are normalized by the single pulse energy level of the matched filter output.

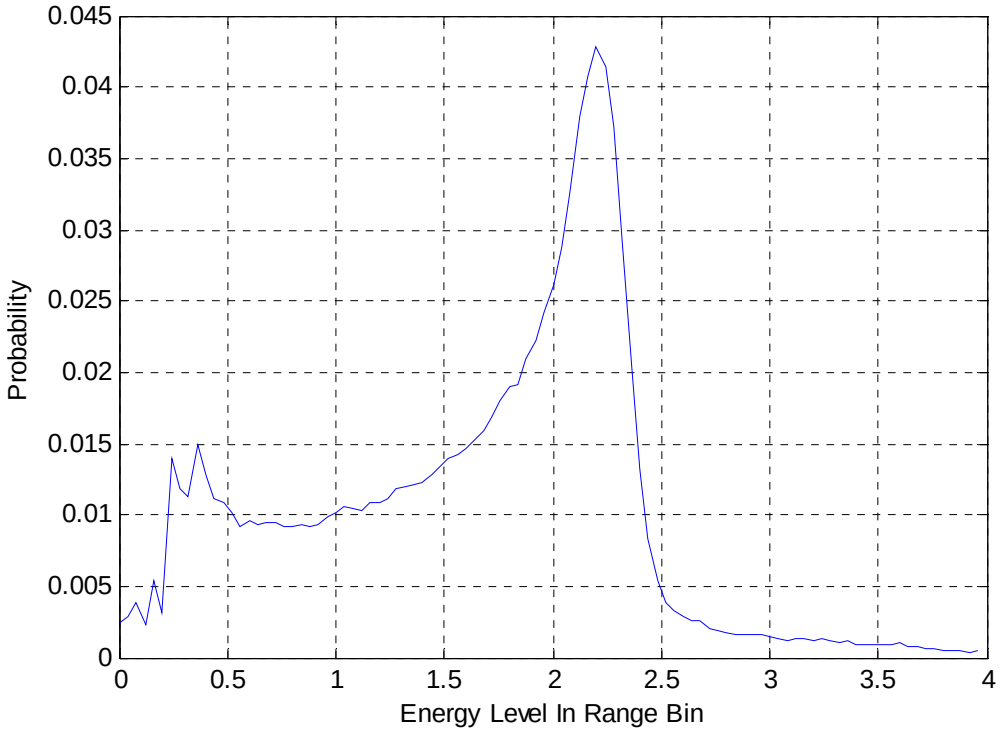

Figure 19-Probability density function for 250 feet trail formation.

Profile #2

In this profile, two-ship trail flight formation is used. The trail distance, dx, is set as 500 feet. Flight parameters for Profile #2 are given in Table 3.

Table 3: Parameters for profile #2.

PROFILE #2 TRAIL	Airspeed First Leg (1.5 min)	Airspeed Second Leg (1 min)	Altitude (feet)	Turn Rate (for 20° check turn)	Trail Distance 'dx' (feet)
Leader	600 K	600 K	10 000	5 deg/min	
Wingman	600 K	600K	10 000	5 deg/min	500

The altitude, trail distance and the airspeed of the flight profile is changed with the values given in Table 3. The total time of the simulation is fixed and 154 seconds. The total energy levels in the range bin of interest for the complete profile #2 is given in Fig. 20. The probability of coherence is given by the ratio of the coherent pair of pulses to total pair of pulses. Therefore, $P[C] = 0.32$ is found with the results given below Fig. 20. Note that the total energy levels after the turn increase drastically while the probability of coherence is low compared to the results from profile #1. It is observed that an initial trail distance of 500 feet yields a higher probability of coherence than the initial trail distance of 250 feet after the turn. On the other hand during the first leg of the profile probability of coherence is significantly higher with a trail distance of 250 feet.

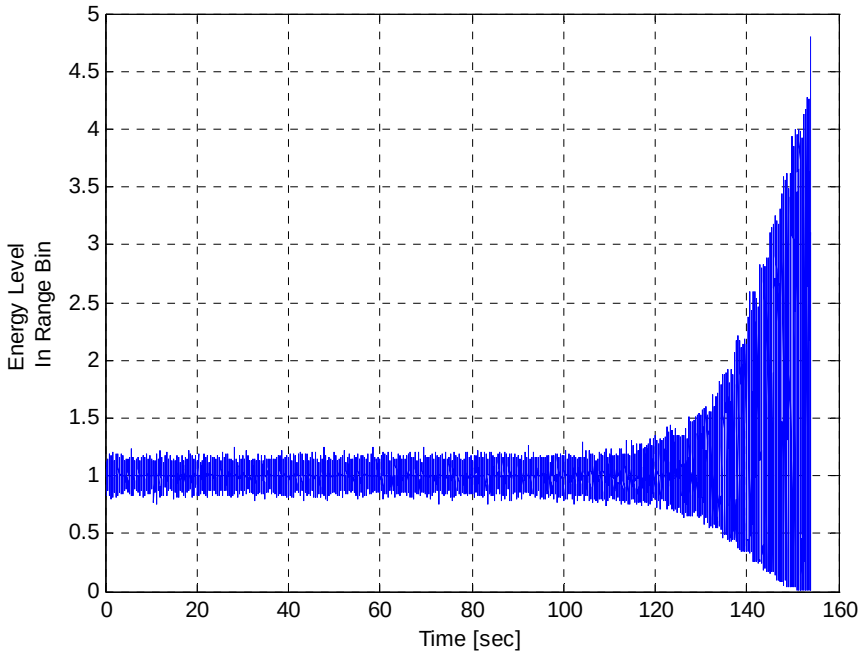

Figure 20: Energy levels in the range bin of interest for each pair of pulses during profile#2 (Number of coherent pair of pulses= 41866, Number of noncoherent pair of pulses= 41495, Number of separate pair of pulses=70639, Number of total pair pulses=154000).

The number of separate pair of pulses is not zero for profile #2. This situation can be observed with the evaluation of the distribution of the first 1540 pair of pulses. Fig. 21 depicts the distribution of the energy levels for the first 1540 pair of pulses for profile #2. Note that this trail distance of 500 feet results 1136 separate pair of pulses out of 1540 pair of pulses during the first leg. When the pulses arrive with a TDOA greater than range bin width, energy level in the range bin of interest reflect the normalized energy level of 1 because only one jamming signal results in the range bin of interest. The second pulse arrives in adjacent range bins depending on the value of TDOA. This situation is also depicted in Fig. 4a where two separate pulses are observed in two different range bins due to the value of TDOA.

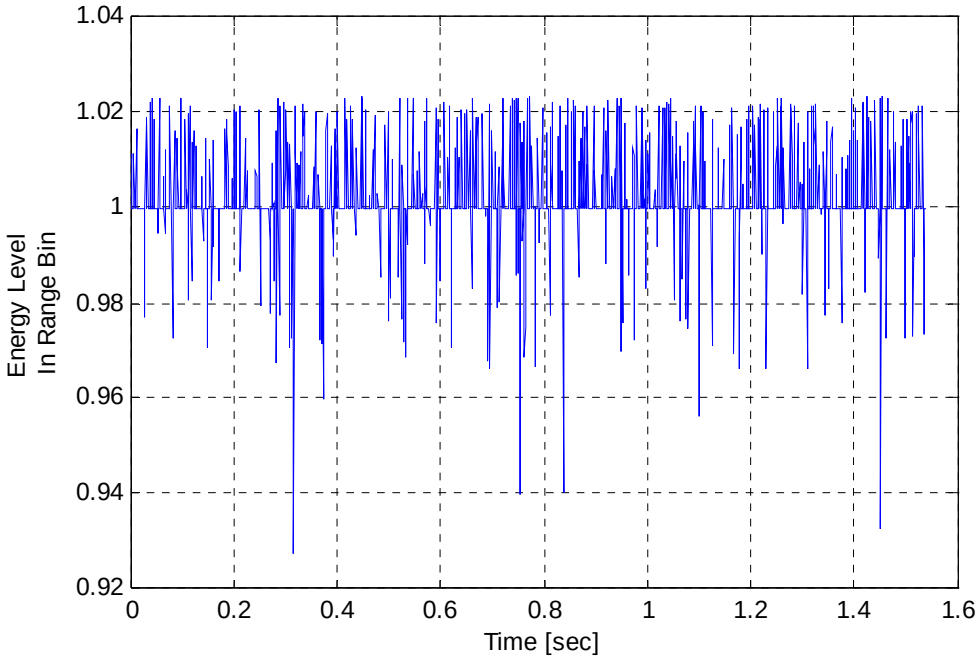

Figure 21: Distribution of the total energy levels in the range bin of interest for profile #2.
(Number of coherent Pulses= 307, Number of Non coherent Pulses= 97, Number of Total Pulses=1540, Number of Separate Pulses=1136).

PDF for the profile #2 is given in Fig. 22 for the observation of the overall distribution of the pulses and the respective probability. Similarly it is possible to evaluate different threshold values for coherence based on the respective probabilities given in Fig. 22. Energy levels in the x-axis are normalized by the single pulse energy level of the matched filter output.

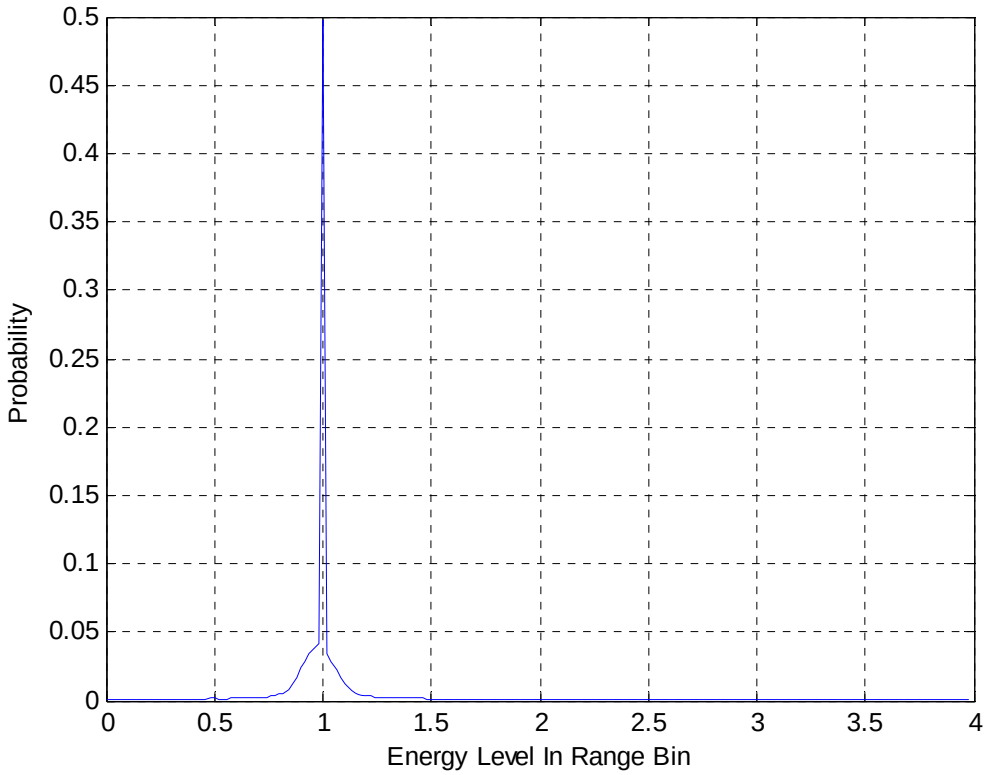

Figure 22- Probability density function for 500 feet trail formation.

Profile #3

This profile is also flown by a two-ship trail flight formation. The trail distance, dx, is set as 750 feet. Flight parameters for profile #3 are given in Table 4.

Table 4: Parameters for profile #3.

PROFILE #3 TRAIL	Airspeed First Leg (1.5 min)	Airspeed Second Leg (1 min)	Altitude (feet)	Turn Rate (for 20° check turn)	Trail Distance 'dx' (feet)
Leader	450 K	450 K	20 000	5 deg/min	
Wingman	450 K	450K	20 000	5 deg/min	750

The altitude, trail distance and the airspeed of the flight profile is changed with the values given in Table 4. The total time of the simulation is fixed and 154 seconds. The total energy levels in the range bin of interest for the complete profile #3 is given in Fig. 23. As seen in the Fig. 23, total energy level in the range bin of interest is reflecting only single jamming pulse because of the trail distance jamming pulses arrive in different range bins. Therefore $P[C] = 0$ is found.

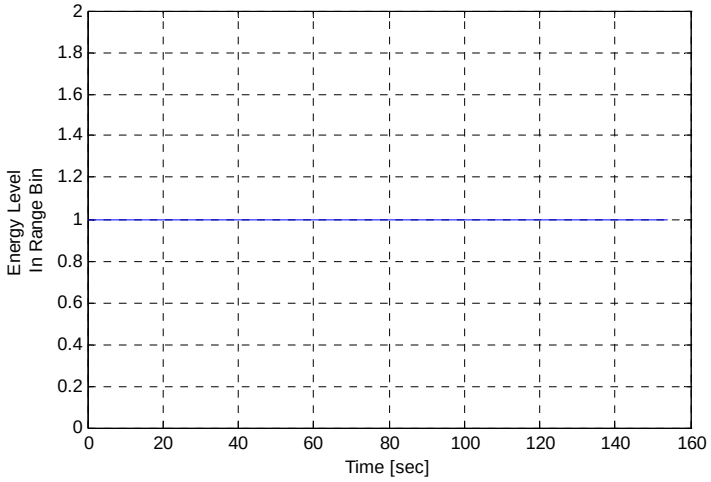

Figure 23: Energy levels in the range bin of interest for each pair of pulses during profile#3 (Number of coherent pair of pulses= 0, Number of noncoherent pair of pulses= 0, Number of seperate pair of pulses=154000, Number of total pair of pulses=154000).

Profile #4

In this profile, two-ship line-abreast flight formation is used. The line-abreast distance, dy, is set as 4000 feet. Flight parameters for profile #4 are given in Table 5.

Table 5: Parameters for profile #4.

PROFILE #4 **LINEABREAST**	Airspeed First Leg (1.5 min)	Airspeed Second Leg (1 min)	Altitude (feet)	Turn Rate (for 20° check turn)	Line abreast Distance 'dy' (feet)
Leader	600 K	600 K	10 000	5 deg/min	
Wingman	600K	600K	10 000	5 deg/min	4000

Line-abreast formation geometry used for the simulation is shown in Fig. 24 as a snapshot from the actual simulation. This visualization is from the beginning of the first leg.

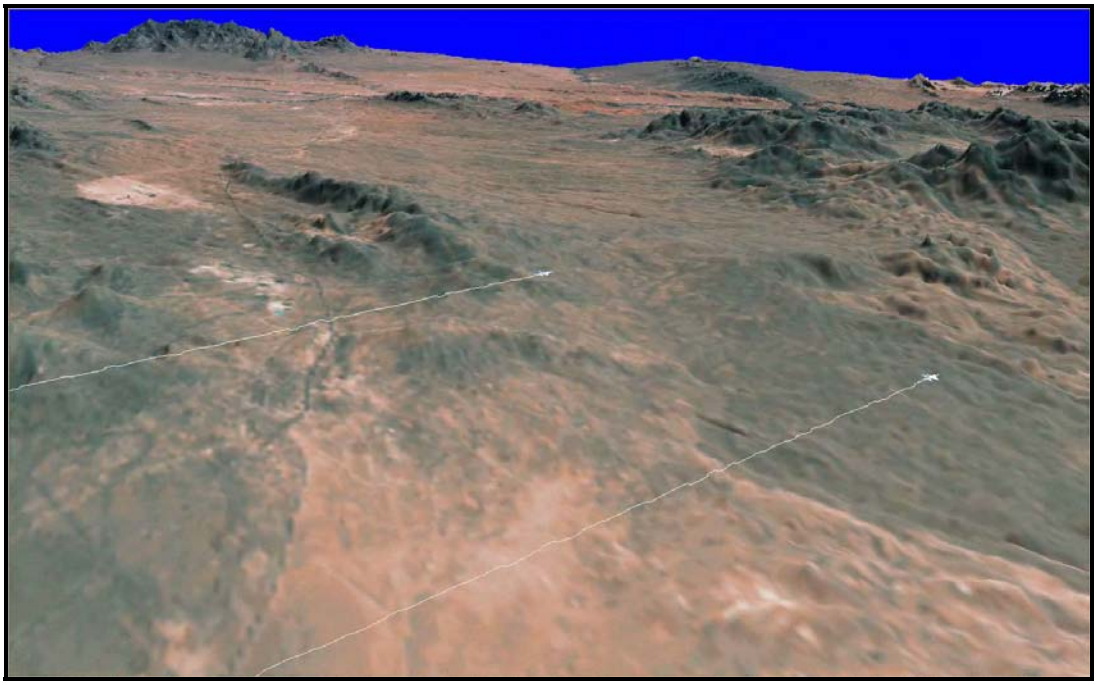

***Figure 24: A snapshot from the beginning of the actual flight profile simulation for visualization of the line abreast formation geometry* [53].**

The top view of the flight profile flown is given in Fig. 25. Similar to trail formation profiles, starting position for the leader aircraft is chosen 25 NM away from the victim radar. Victim radar location is defined as the origin for the simulation. Total flight profile is lasted for 154 seconds. First leg is flown for 90 seconds followed by a $20°$ check turn which is completed in 4 seconds. Second leg is flown for 60 seconds.

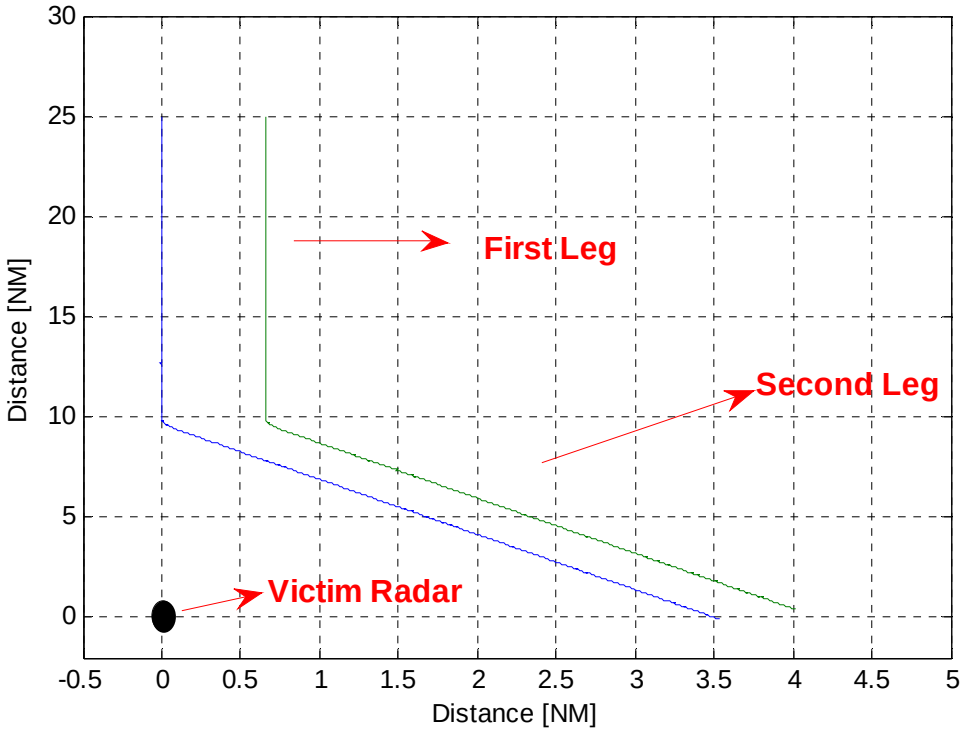

Figure 25: Top view for the complete profile #4.

Both aircraft initiated the check turn at time $t = 90\,\text{s}$ and this resulted in a line-abreast formation geometry where the wingman is in a relatively forward position compared to initial line-abreast position in the first leg. Fig. 26a is snapshot visualization from the actual simulation showing the simultaneous initiation of the check turn by both

aircraft. The resulting formation geometry described above can be observed in Fig. 26b. The airspeed of the wingman and the leader kept equal and constant as given in Table 5.

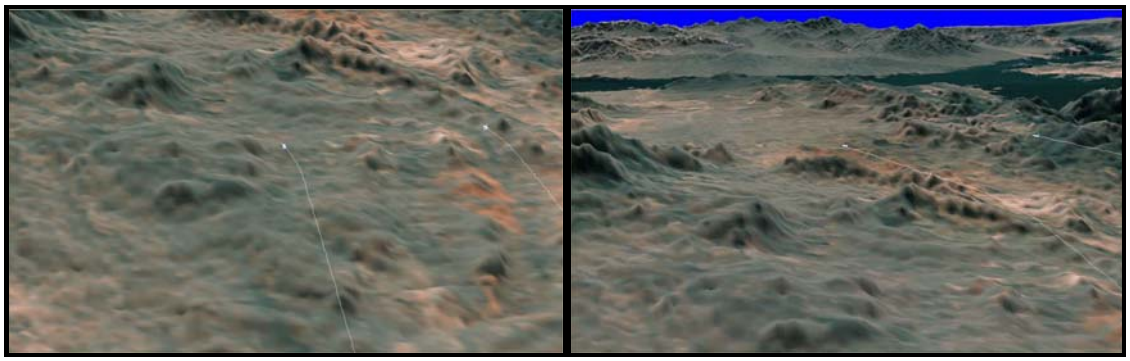

(a) (b)

***Figure 26: Check turn and the line-abreast formation is distorted from the initial setup parameters* [53].**

Similarly, the coherence of jamming signals for the complete profile is evaluated. Using the coherence model that is developed in Chapter IV, the total energy levels for the 154 000 pair of pulses are found and shown in Fig. 27. A summary of the resulting coherence is given below Fig. 27. The probability of coherence is given by the ratio of the coherent pair of pulses to total pair of pulses. Therefore $P[C] = 0.40$ is found with the results given below Fig. 27. This probability of coherence is calculated for the entire profile.

However it must be noted from Fig. 27 that the pair of pulses arrive in separate range bins mostly after the turn. For the specific time interval the probability of coherence is given by the ratio of the coherent pair of pulses to total pair of pulses. This implies that the overall probability of coherence for the entire flight path can be misleading in many cases.

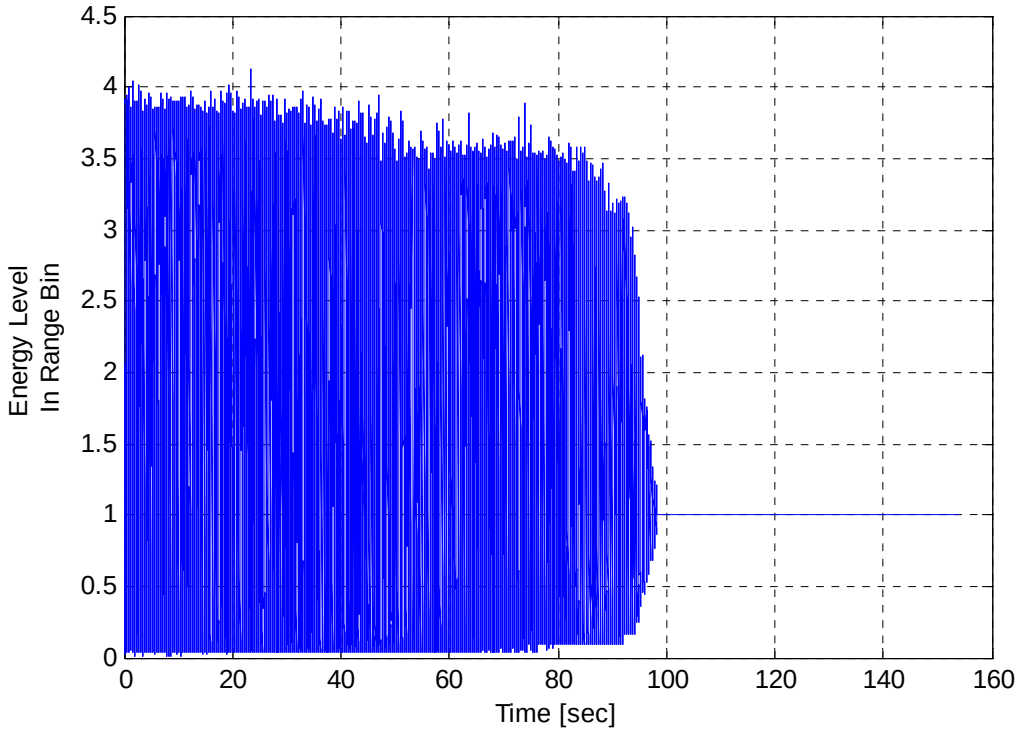

Figure 27: Energy levels in the range bin of interest for each pair of pulses during profile#4 (Number of coherent pair pulses= 61214, Number of noncoherent pair of pulses= 36944, Number of separate pair of pulses=55842, Number of total pair of pulses=154000).

Probability density function for profile #4 is given in Fig. 28. Note that $P[C]$ can be calculated for different threshold values because any energy level can be set as a threshold for coherence and the respective probability for coherence can be evaluated from Fig. 28. Energy levels in the x-axis are normalized by the single pulse energy level of the matched filter output.

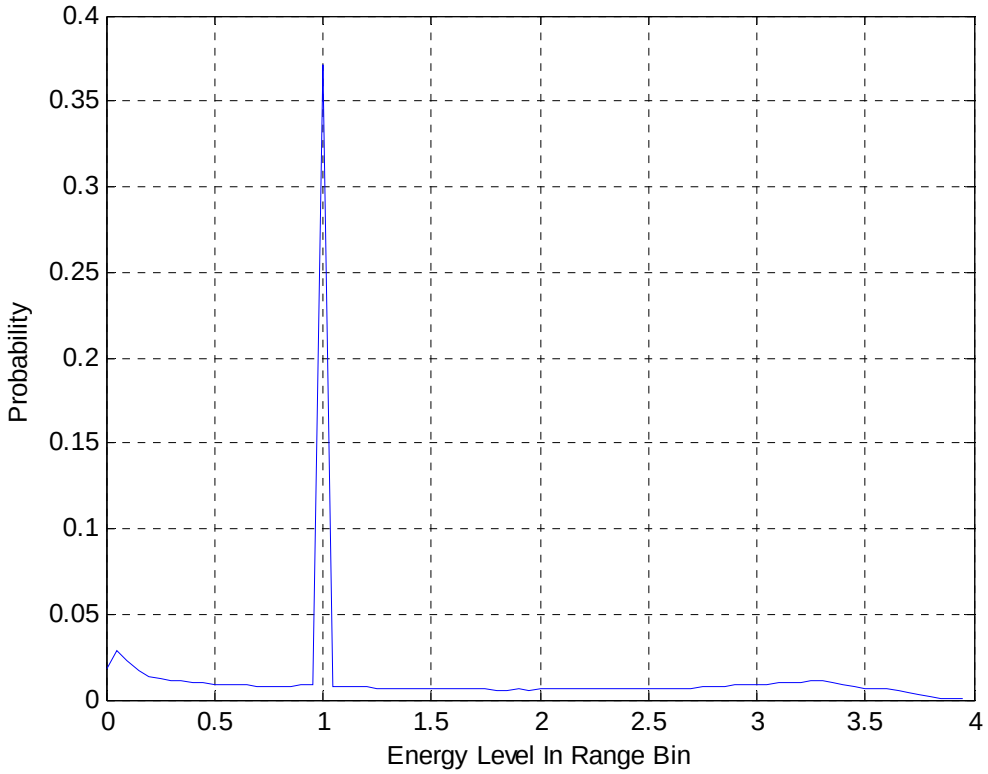

Figure 28: Probability density function for 4000 feet line abreast formation.

Profile #5

In this profile is also flown as a two-ship line-abreast flight formation. The line-abreast distance, dy, is set as 5000 feet. Flight parameters for Profile #5 are given in Table 6. Note that in this profile, the airspeed for the wingman is decreased by 30 K in the second leg with an attempt to preserve initial formation geometry after the turn.

Table 6: Parameters for Profile #5.

PROFILE #5 **LINEABREAST**	Airspeed First Leg (1.5 min)	Airspeed Second Leg (1 min)	Altitude (feet)	Turn Rate (for 20° check turn)	Line abreast Distance 'dy' (feet)
Leader	500 K	500K	15 000	5 deg/min	
Wingman	500K	470K	15 000	5 deg/min	5000

The altitude, line-abreast distance and the airspeed of the flight profile is changed with the values given in Table 6. The total time of the simulation is fixed and 154 seconds. The total energy levels in the range bin of interest for the complete profile #5 are given in Fig. 29. The probability of coherence is given by the ratio of the coherent pair of pulses to total pair of pulses. Therefore, for the duration of the entire profile, $P[C] = 0.43$ is found with the results given below Fig. 29.

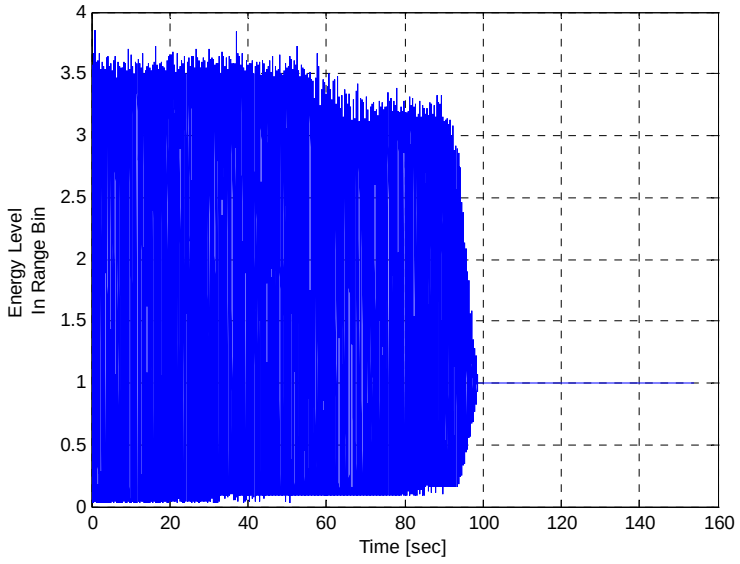

Figure 29: Energy levels in the range bin of interest for each pair of pulses during profile#4
(Number of coherent pair pulses= 66188, Number of noncoherent pair of pulses= 32053, Number of separate pair of pulses=55759, Number of total pair of pulses=154000).

Probability density function for profile #5 is given in Fig. 30. Similarly different energy levels can be set as a threshold for coherence and the respective probability for coherence can be evaluated for this profile as well.

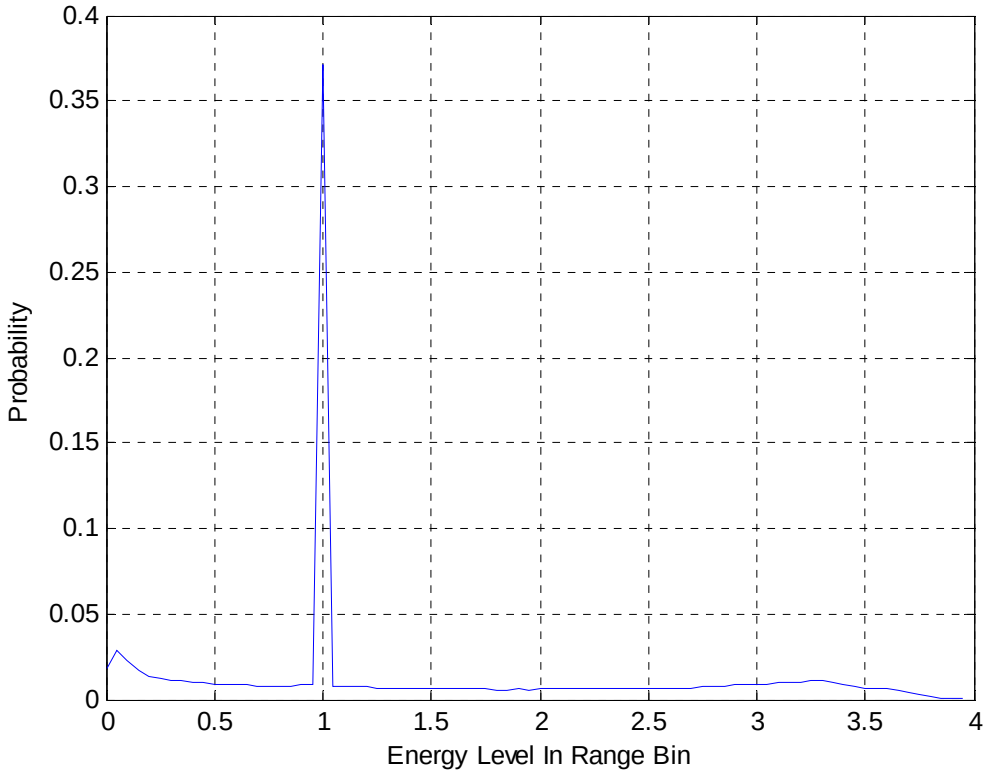

Figure 30: Probability density function for 5000 feet line abreast formation.

Profile #6

This profile is also flown as a two-ship line abreast flight formation. The line abreast distance, dy, is set as 6000 feet. Flight parameters for profile #6 are given in Table 7. Note that in this profile, similar to the profile #5, the airspeed for the wingman is decreased by 30 K in the second leg with an attempt to preserve initial formation geometry after the turn.

Table 7: Parameters for profile #6.

PROFILE #6 **LINEABREAST**	Airspeed First Leg (1.5 min)	Airspeed Second Leg (1 min)	Altitude (feet)	Turn Rate (for 20° check turn)	Line abreast Distance 'dy' (feet)
Leader	450 K	450K	10 000	5 deg/min	
Wingman	450K	420K	10 000	5 deg/min	6000

The total energy levels in the range bin of interest for the complete profile #6 are given in Fig. 31. The probability of coherence is given by the ratio of the coherent pair of pulses to total pair of pulses. Therefore, for the duration of the entire profile, $P[C] = 0.38$ is found with the results given below Fig. 31.

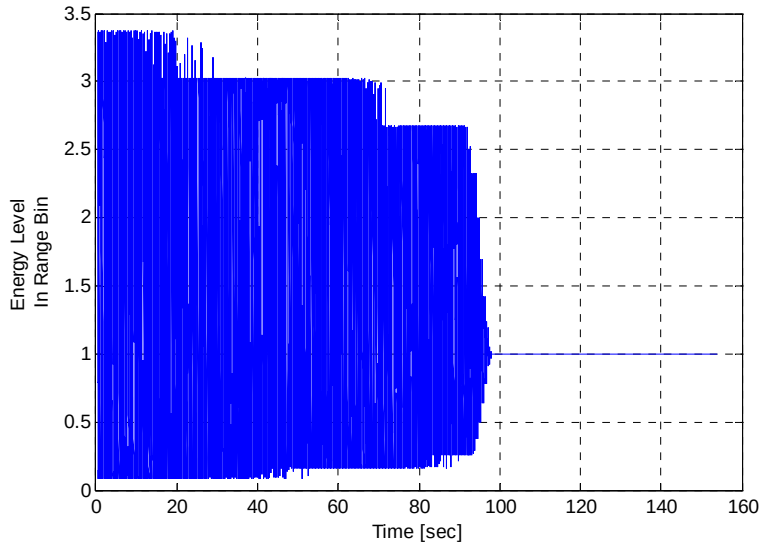

Figure 31: Energy levels in the range bin of interest for each pair of pulses during profile#6
(Number of coherent pair pulses= 58674, Number of noncoherent pair of pulses= 38938, Number of separate pair of pulses=56388, Number of total pair of pulses=154000).

Probability density function for profile #5 is given in Fig. 32. Similarly different energy levels can be set as a threshold for coherence and the respective probability for coherence can be evaluated for this profile as well.

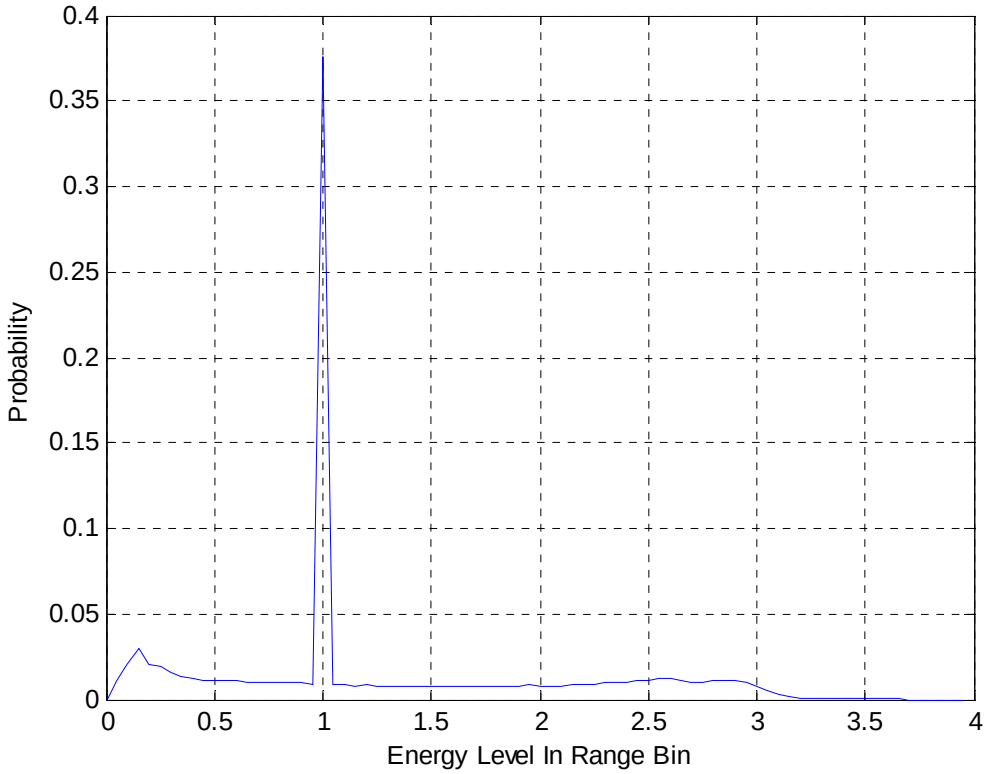

Figure 32: Probability density function for 6000 feet lineabreast formation.

VI. Results

Result 1

Impact of flight path and formation geometry on the coherence of jamming signals is verified through modeling and simulation. Different probability of coherence values are found for different flight paths and formation geometries. This outcome verified the existence of an interactive relationship between flight path and formation geometry and the EW effectiveness.

Result 2

Evaluation of the nature of this interactive relationship in six different flight profiles revealed that specific flight paths and formation geometries can be designed during the mission planning processes to enhance the jamming effectiveness. The nature of the results arrived in Chapter V dictates that the formation geometry should be designed for the specific time period of the flight profile. Because it is observed that the overall probability of coherence for the entire flight profile may be misleading. For instance, a line abreast formation yielded higher probability of coherence in the initial leg of the flight profile while a fighting wing formation yielded higher probability of coherence in the second leg of the flight profile.

Result 3

The location of the victim radar is verified to be the vital input in deciding the instantaneous formation geometry of the tactical formation during the engagement. With this information available, mission planning processes may produce proper formation

geometry and flight path to increase the survivability. This result implies that the hypothesis postulated in the beginning of the research is valid provided that the all vital inputs are present during the mission planning. Applications of the results are further discussed from the perspective of survivability in the next section.

Application of the Results

The results imply that the quasi-coherent effects caused by two self-protection jammers can create stronger false targets in the radar receiver. Hence, the false target can degrade the threat radar's capability to track and launch threat missiles at the aircraft increasing aircraft survivability. The next stage of this work is to develop a model for probability of survival based on probability of coherence. The analysis of the engagement level survivability can be visualized as a tree diagram shown in Fig. 32. Similar methodology for "mission level survivability" can be found in [22].

In order for the threat weapon system to kill the aircraft at the end of the engagement, the flow of the events $\mathbb{R}$ and $\mathbb{Z}$ must follow the solid arrows on the right. Probability of Survival, P_S, is the complement of the Probability of Kill, P_K, and two events have mutually exclusive and exhaustive outcomes [22]. It should be noted that Fig. 32 is drawn for "non-coherent EA". When the same analysis is carried out for the engagement where "coherent EA" is implemented (assuming that all other factors remain constant) the resulting new probability of kill may be expressed in terms of the original P_K as

$$P_K^{'} = \alpha P_K \tag{30}$$

where $P_K = P[\mathbb{Z}\,|\,\mathbb{R}]P[\mathbb{R}]$. Therefore, the probability of survival for coherent EA is $P_S^{'} = 1-\alpha P_K$.

The scaling factor α reflects the impact of coherent EA on the survivability. It is then possible to decide the increase in survivability of a strike formation through coherent self-protection jammers.

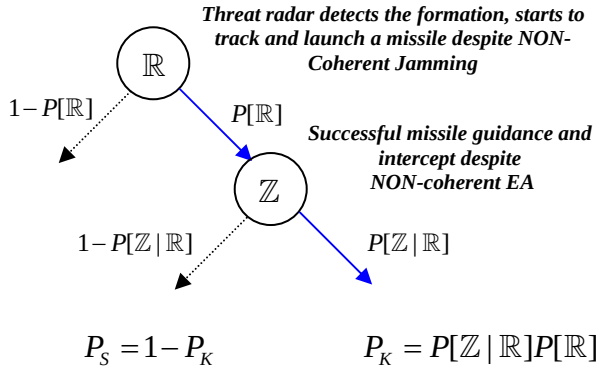

Figure 32: Probability of survival tree diagram.

VII. Conclusions and Future Work

Conclusion

This preliminary experiment revealed that it is possible to measure the impact of coherent jamming on combat aircraft survivability through the method of difference. The evaluation of basic tactical formation geometries and flight paths from the perspective of jamming effectiveness proved that proper mission planning may increase the total survivability. These positive results can be viewed as a motivation to conduct more extensive research with a high fidelity tracking radar model and a flight simulation which includes an atmospheric model.

Future Work

The application of interconnection of the coherent SPJ jammers via a data link to exchange processed data may be explored from the perspective of sensor fusion techniques. The advantages of sensor fusion applications such as the datalink between the airborne radars of tactical aircraft are briefly discussed in [1]. Cooperative tactical operations that use a data link can be organized into three categories: situation awareness (threat tracking, system status), offensive operations (attack planning, missile handoff), defensive operations (EW, missile warning) [55]. This study can be further evaluated in all three categories mentioned above. The future research may also shift its tactical perspective from manned aircraft to Unmanned Combat Aircraft Vehicle (UCAV) and respective sensor fusion application opportunities as well.

References

[1] F. Neri, *Introduction to Electronic Defense Systems.* Norwood, MA: Artech, 2001.
[2] M. I. Skolnik, *Radar Handbook.* New York: Mc Graw Hill, 1990.
[3] D. C. Scheler, *Electronic Warfare in Information Age.* Norwood, MA: Artech House, 1989.
[4] M. Dewar, *The Art of Deception in Warfare.* Park Avenue, New York: Steling Publishing Co. Inc., 1989.
[5] *Military Handbook: Aircraft Survivability.* MIL-HDBK-2069, Department of Defense, United states of America, 1997.
[6] O. Regev, "With static and sword: Part I: The offensive EW concept: Tactical aircraft must take the offensive against future threats," *Journal of Electronic Defense* 24, no.12, pp. 45-46, Dec. 2001.
[7] M. J. Foley, and S. G. Gress, "A Simulation model to evaluate aircraft survivability and target damage during offensive counter air operations," M.S. Thesis, Air Force Institute of Technology, OH, 1984.
[8] M. D. Reid, "Survivability of interdiction aircraft: Sensitivity to terrain following, command altitude, velocity, and electronic counter measures," M.S. Thesis, Air Force Institute of Technology, OH, 1984.
[9] *Jane's Radar and Electronic Warfare Systems 2007-2008, 19th ed.,* Jane's Information Group Limited, Alexandria, VA, 2007.
[10] M. I. Skolnik, *Introduction to Radar Systems.* New York: Mc Graw Hill, 2001.
[11] D. K. Barton, *Radar System Analysis and Modeling.* Norwood, MA: Artech House, 2005.
[12] L. B. Van Brundt, *Applied ECM, vol. III.* VA: Electronic Warfare Engineering, Inc., 1995.
[13] F. Kural, and Y. Ozkazanc, "A method for detecting RGPO/VGPO jamming/ RGPO/VGPO karistirmasinin sezimi icin bir yontem," in *Proc. IEEE 12th Signal Processing and Communication Applications Conf.* pp. 237-240, 2004.
[14] E. J. Chrzanowski, *Active Radar Electronic Countermeasures.* Norwood, MA: Artech House, 1990.
[15] L. B. Van Brundt, *Applied ECM, vol. I.* VA: Electronic Warfare Engineering, Inc., 1978.
[16] L. B. Van Brundt, *Applied ECM, vol. II.* VA: Electronic Warfare Engineering, Inc., 1978.
[17] C. Zhongfei, "Effects of Range Gate Pull-Off (RGPO) Jamming On Some Pulse Radars," *Aerospace Shanghai*, vol. 12, pp. 23-26, Oct. 1996.
[18] R. P. Hallion, "A Short History of Aircraft Survivability," *Aircraft Survivability,* pp. 10-13, Summer 2001.
[19] S. Budiansky, *Air Power.* New York: Penguin Books, 2004.
[20] J. Matsumura, R. Steeb, B. Crowe, N. Dienna, Y. Huh, G. Quintero, W. Solfrey, "Survivability options for maneuver and trasport aircraft," RAND Arroyo Center, Santa Monica, CA: RAND Corporation, 2004.
[21] Committee on Future Air Force Needs for Survivability, "Future Air Force needs for survivability," National Research Council of The National Academies, Washington, D.C. : The National Academies Press, 2006.
[22] R. B. Ball, *The Fundamentals of Aircraft Combat Survivability Analysis and Design.* Monterey, CA: American Institute of Aeronautics Inc., 2003.
[23] J. F. O'Bryon, "Tearing the Walls Down to Achieve Greater Aircraft Survivability," *Aircraft Survivability,* pp. 7-11, Summer 2000.
[24] B. Hood, "Vulnerability Reduction," *Aircraft Survivability*, pp. 7-9, Spring 2006.
[25] M. W. Dinning and B. S. Tenney, "Army S&T Program for Aircraft Survivability," *Aircraft Survivability*, pp. 28-29, Summer 2001.
[26] J. Heikell, "Electronic warfare self-protection of battlefield helicopters: A holistic view," Ph.D. dissertation, Dept. Elect. Eng., Helsinki Univ., Espoo, Finland, 2005.
[27] R. J. Schlesinger, *Principles of Electronic Warfare.* Englewood Cliffs, NJ: Prenticehall, 1961.
[28] S. Mulgund, K. Harper, K. Krishnakumar, and G. Zacharias, "Air combat tactics optimization using stochastic genetic algorithms," in *IEEE International Conference on Systems, Man, and Cybernetics*, San Diego, CA, USA, vol.4, pp. 3136-3141, 1998.
[29] L. H. McKenna, S. Little, "Developing tactics using low cost, accessible simulations" in *Proc. 2000 IEEE Winter Simulation Conference,* Orlando, FL, USA, pp. 991-1000, 2000.
[30] S. Glaerum, "TALUS-an object oriented air combat simulation" in *Proc. 1999 IEEE Winter Simulation Conference*, Phoenix, AZ, USA, vol.2, pp. 1160-1167, 1999.
[31] A. M. Graziano, *Research Methods.* Boston, MA: Pearson Education Group, 2004.
[32] W. C. Booth, G. G. Colomb, and J. M. Williams, *The Craft of Research.* Chicago, IL: The University of Chicago Press, 2003.
[33] R. V. Smith, *Graduate Research,* New York, NY: Plenum Press, 1990.
[34] S. Ozer, M. A. Saville, P. J. Collins, A. J. Terzuoli, "Modeling of a strike formation with coherent self-protection jammers," 2008 IEEE Radar Conference, Rome, Italy May 2008.
[35] D. L. Adamy, *Introduction to Electronic Warfare Modeling and Simulation.* Raleigh, NC: SciTech, 2006.
[36] B. P. Lathi, *Signals Processing &Linear Systems.* NY: Oxford University Press, 1998.
[37] G. R. Curry, *Radar System Performance Modeling.* Norwood, MA: Artech House, 2005.
[38] S. A. Leonov, and A. I. Leonov, *Handbook of computer Simulation In Radio Engineering, Communication, and Radar.* Norwood, MA: Artech House, 2001.
[39] M. J. Beran, and G. B. Parrent, Jr., *Theory of Partial Coherence.* Englewood Cliffs, NJ: Prentice-Hall, 1964.
[40] G. W. Stroke, *An Introduction to Coherent Optics and Holography.* New York: Academic Press, 1966.
[41] M. Golio, *RF and Microwave Handbook.* Boca Raton, FL: CRC Press, 2001.
[42] G. W. Stimson, *Introduction to Airborne Radar.* Menham, NJ: Scitech Publishing, 1998
[43] R. N. Lothes, M. B. Wiley and G. Richard, *Radar Vulnerability to Jamming.* Boston, MA: Artech House, 1990.
[44] S. A. Vakin, L. N. Shustov, and R. H. Dunwell, *Fundamentals of Electronic Warfare.* Norwood, MA: Artech House, 2001.
[45] J. C. Toomay, *Radar Principles for the non-Specialists.* Raleigh, NC: SciTech, 2004.
[46] G. W. Deley, :Waveform Design," in M. I. Skolnik, *Radar Handbook.* New York: Mc Graw Hill, 1970.

[47] T. S. ElAli, and M. A. Karim, *Continuous Signals and Systems with MATLAB.* Boca Raton, FL: CRC Press, 2001.
[48] R. A. Poisel, *Target Acquisition in Communication Electronic Warfare Systems.* Norwood, MA: Artech House, 2004.
[49] R. Schapiro, *ABC's of Missile Guidance.* Indianapolis, IN: Howard W. Sams &Co., 1962.
[50] A. S. Locke, *Guidance.* New York, NY: D. Van Nostrand Company, 1955.
[51] A. L. Garcia, *Probability and Random Processes for Electrical Engineering.* MA: Addison- Wesley Publishing Company, 1994.
[52] R. L. Shaw, *Fighter Combat Tactics and Maneuvering.* Annapolis, MD: Naval Institute, 1985.
[53] P. A. Blue and M. W. Coldsnow, "Flight Simulator," unpublished .
[54] L. T. Nguyen, et al. "Simulator Study of Stall/Post-Stall Characteristics of a Fighter Airplane with Relaxed Longitudinal Static Stability." NASA Tech Paper 1538. Washington DC, NASA, December 1979.
[55] M. Beach, "Cooperative tactical operations using a data link," in *1990 Proc. IEEE/AIAA/NASA 9th Digital Avionics Systems Conference,* Virginia Beach, VA, USA, pp. 549-551, Oct 1990.

REPORT DOCUMENTATION PAGE

Form Approved
OMB No. 074-0188

1. REPORT DATE *(DD-MM-YYYY)*	**2. REPORT TYPE**	**3. DATES COVERED** *(From – To)*
27-03-2008	Master's Thesis	August 2006 – March 2008

4. TITLE AND SUBTITLE

INCREASING COMBAT AIRCRAFT SURVIVABILITY THROUGH COHERENT SLEF-PROTECTION JAMMERS

5a. CONTRACT NUMBER

5b. GRANT NUMBER

5c. PROGRAM ELEMENT NUMBER

6. AUTHOR(S)

ÖZER, Soner, 1st.Lt, TuAF

5d. PROJECT NUMBER
If funded, enter ENR #

5e. TASK NUMBER

5f. WORK UNIT NUMBER

7. PERFORMING ORGANIZATION NAMES(S) AND ADDRESS(S)
Air Force Institute of Technology
Graduate School of Engineering and Management (AFIT/EN)
2950 Hobson Way, Building 640
WPAFB OH 45433-8865

8. PERFORMING ORGANIZATION REPORT NUMBER

AFIT/GE/ENG/08-20

9. SPONSORING/MONITORING AGENCY NAME(S) AND ADDRESS(ES)
Paul Howland
Surveillance & Reconnaisance Resource Center NATO C3 Agency +31703743752 Paul.Howland@nc3a.nato.int

10. SPONSOR/MONITOR'S ACRONYM(S)

11. SPONSOR/MONITOR'S REPORT NUMBER(S)

12. DISTRIBUTION/AVAILABILITY STATEMENT

APPROVED FOR PUBLIC RELEASE; DISTRIBUTION UNLIMITED.

13. SUPPLEMENTARY NOTES

14. ABSTRACT

When the battlefields were within the visual range, the objective of deception tactics in warfare was to deceive the human senses. In the battlefield of electromagnetic spectrum, the objective of deception is to deceive the sensors of the enemy weapon systems.

The survivability of the aircraft operating in hostile environment is of prime importance to the mission planner. If the aircraft can deny its location information to the tracking radar of the radar guided threat missile system, this, in return, may increase its survivability. The deception, a tactic which stems from the wisdom of ancient battles, incarnated in the form of Electronic Attack (EA) can give this capability to the aircraft operating in a hostile environment. Self-Protection Jammers (SPJs) mounted on aircraft that employ deception-repeater jamming techniques and the resulting effect of the deception jamming on the enemy sensor systems will be examined in this study.

The impact of the specific flight path and formation geometry should be considered both from the perspective of coherent SPJs effectiveness and the survivability. The individual effectiveness of the EA by SPJs is usually limited by the available Effective Radiated Power (ERP). Due to limitations on the size of the aircraft, one can not afford to build powerful SPJs. The jamming technique and the effect of multiple jammers with respect to jamming effectiveness need to be examined for mission planning analysis. The specific jamming technique evaluated is the combined Range Gate Pull-Off (RGPO) and Velocity Gate Pull-Off (VGPO) against pulse Doppler radar.

The challenge is to decide the least vulnerable flight path and the formation geometry for a strike formation in an air-to-ground engagement scenario. The degree of survivability provided by the combination of the formation geometry, flight path and the EA (multiple spatially dispersed coherent jammers) is the focus of this research. The modeling and simulation of the interactions between the self-protection jammer and the pulse Doppler tracking radar with respect to formation geometry and flight path is the initial objective.

15. SUBJECT TERMS
Combat Survivability, Self-Protection Jamming, Coherence of Jamming Signals.

16. SECURITY CLASSIFICATION OF:			**17. LIMITATION OF ABSTRACT**	**18. NUMBER OF PAGES**	**19a. NAME OF RESPONSIBLE PERSON**
a. REPORT	**b. ABSTRACT**	**c. THIS PAGE**			Saville, Michael A. Maj. USAF.
U	U	U	UU	75	**19b. TELEPHONE NUMBER** *(Include area code)* (937) 2553636-4219 (Michael.Saville@afit.af.edu)

Standard Form 298 (Rev. 8-98)
Prescribed by ANSI Std. Z39-18